Journal of the Endocrine Society, 2022, **6**, 1–18
https://doi.org/10.1210/jendso/bvac082
Advance access publication 19 May 2022
Research Article

ANGT_HUMAN[448–462], an Anorexigenic Peptide Identified Using Plasma Peptidomics

Sayaka Sasaki,[1] Kazuhito Oba,[1] Yoshio Kodera,[2,3] Makoto Itakura,[4] and Masayoshi Shichiri[1,5]

[1]Department of Endocrinology, Diabetes and Metabolism, Kitasato University School of Medicine, Kanagawa 252-0374, Japan
[2]Department of Physics, Kitasato University School of Science, Kanagawa 252-0373, Japan
[3]Center for Disease Proteomics, Kitasato University School of Science, Kanagawa 252-0373, Japan
[4]Department of Biochemistry, Kitasato University School of Medicine, Kanagawa 252-0374, Japan
[5]Department of Diabetes, Endocrinology and Metabolism, Tokyo Kyosai Hospital, Tokyo 153-8934, Japan

Correspondence and Reprint Requests: Masayoshi Shichiri, MD/PhD, 2-3-8, Nakameguro, Meguro-ku, Tokyo 153-8934, Tokyo Kyosai Hospital, Tokyo 153-8934, Japan. Email: shichiri@tkh.meguro.tokyo.jp

Abstract

The discovery of bioactive peptides is an important research target that enables the elucidation of the pathophysiology of human diseases and provides seeds for drug discovery. Using a large number of native peptides previously identified using plasma peptidomics technology, we sequentially synthesized selected sequences and subjected them to functional screening using human cultured cells. A 15-amino-acid residue proangiotensinogen-derived peptide, designated ANGT_HUMAN[448–462], elicited cellular responses and bound to cultured human cells. Synthetic fluorescent-labeled and biotinylated ANGT_HUMAN[448–462] peptides were rendered to bind to cell- and tissue-derived proteins and peptide-cell protein complexes were retrieved and analyzed using liquid chromatography–tandem mass spectrometry, revealing the β-subunit of ATP synthase as its cell-surface binding protein. Because ATP synthase mediates the effects of anorexigenic peptides, the ability of ANGT_HUMAN[448–462] to modulate eating behavior in mice was investigated. Both intraperitoneal and intracerebroventricular injections of low doses of ANGT_HUMAN[448–462] suppressed spontaneous food and water intake throughout the dark phase of the diurnal cycle without affecting locomotor activity. Immunoreactive ANGT_HUMAN[448–462], distributed throughout human tissues and in human-derived cells, is mostly co-localized with angiotensin II and is occasionally present separately from angiotensin II. In this study, an anorexigenic peptide, ANGT_HUMAN[448–462], was identified by exploring cell surface target proteins of the human native peptides identified using plasma peptidomics.

Key Words: ANGT_HUMAN[448–462], angiotensinogen, food intake, liquid chromatography–tandem mass spectrometry, plasma peptidomics, anorectic peptide

Abbreviations: ANOVA, analysis of variance; ATP5B, human ATP synthase β-subunit; CN-PAGE, clear-native polyacrylamide gel electrophoresis; FDR, false discovery rate; GH3, rat pituitary tumor cells; HAoECs, human aortic endothelial cells; HCT116, human colorectal carcinoma cells; HEK293, human embryonic kidney cells; HeLa, human uterine cervical carcinoma cells; HRP, horseradish peroxidase; HUEhT-1, human umbilical vascular endothelial cells; LC-MS/MS, liquid chromatography–tandem mass spectrometry; PAGE, polyacrylamide gel electrophoresis; PBS, phosphate-buffered saline; PEP, posterior error probability; PSM, peptide spectrum match; Rat-1, rat fibroblast cell line; RD, human rhabdomyosarcoma cells; SEM, standard error of the mean; siATP5B, siRNA against human ATP synthase β-subunit; siRNA, small interfering RNA; TFA, trifluoroacetic acid; THP1, human monocytic leukemia cell line; UV♀2, RCB1994 UV-induced angioendothelioma-like tumor mouse cell line; XIC, extracted ion chromatogram.

Despite the anticipation that human plasma contains unidentified, biologically active factors involved in normal human physiology and disease pathophysiology, a limited number of human bioactive peptides have been discovered during the past 2 decades. This was primarily due to the unavailability of advanced technology to identify, in human plasma, low-molecular-weight native peptides, which are present at extremely low concentrations and are buried in a vast amount of far larger constituent plasma proteins [1, 2]. For example, the plasma levels of potent bioactive peptides, such as natriuretic peptides and angiotensin II, are usually less than 40 and 20 pg/mL, respectively, which are 10^9 orders of magnitude lower than those of serum albumin and immunoglobulin G. Efficient removal of such high-abundance plasma proteins and enrichment of the myriad of unidentified low-abundance native peptides to the levels required for their identification using mass spectrometry poses a great challenge, leaving potential unidentified bioactive/biomarker peptides and deorphanized G protein-coupled receptors. We recently succeeded in establishing an improved technology to enrich plasma low-molecular-weight peptides with extremely high efficiency to levels that allow their comprehensive identification using liquid chromatography–tandem mass spectrometry (LC-MS/MS) without digesting plasma with trypsin [3, 4]. We previously identified a large number of plasma native peptides from a single drop of human blood, and the results were deposited into the human plasma native peptidomic database [5].

We performed *in silico* analysis of this peptidomic resource to select peptides for initial functional screening, chemically synthesized the sequences, and, after confirming the high purity and high solubility of the synthetic peptides using LC-MS/MS, tested their ability to elicit intracellular signaling in in vitro analyses [5]. In the present study, we attempted to identify surface target proteins of peptides that induced cell responses and showed significant binding to the cell surface

Received: 30 December 2021. **Editorial Decision:** 17 May 2022. **Corrected and Typeset:** 9 June 2022

through initial in vitro screening. Synthetic peptides were rendered to bind to putative cell surface-binding proteins/receptors, and the cross-linked cell membrane proteins were eluted and directly analyzed using LC-MS/MS. The identified cell surface target proteins may allow the estimation of their potential biological activities, and this strategy has successfully resulted in the identification of a new biologically active peptide.

Materials and Methods

In Silico Selection of Peptides From Native Plasma Peptidomic Resource

We used the human plasma native peptidomic resource that we previously identified using LC-MS/MS. Our initial acquisition data were searched against the SwissProt_2015_02.fasta database using 2 different data-processing pipelines and search engines: Mascot Distiller (version 2.5.1.0, Matrix Science) and PEAKS Studio (version 7). All polypeptide sequences classified with peptide identification false discovery rates (FDRs) of 1%, except for those derived from the keratin protein family, were deposited into the ProteomeXchange Consortium via the PRoteomics IDEntifications (PRIDE) [6] partner repository with the dataset identifier PXD003533. This resource was later re-analyzed using PEAKS Studio (version X) based on a de novo sequencing-based database search using the SwissProt_2020_03.fasta database with 5 variable post translational modifications in addition to carbamidomethylation, and not using the peptide spectral match (PSM) algorithm, resulting in the identification of 7959 distinct native peptide sequences with FDRs of 0% [5]. The peptide library was analyzed *in silico* to select peptides for subsequent functional screening studies using the following criteria: (i) uniquely assigned to a precursor protein family, (ii) assigned a gene name or a gene name of a protein family, (iii) encoded by secretory proteins as defined by SwissProt keywords, (iv) amino acid lengths of 5–38 residues, (v) no substitutions or modifications except for C-terminal amidation, (vi) no cysteine residues, (vii) potential extracellular release predicted using a bioinformatics tool, PSORT [7], and (viii) identified with an FDR of 0%. Selected peptides were chemically synthesized (Scrum Inc., Tokyo, Japan) and reconstituted to 2 to 10×10^{-3} M with 10% acetonitrile/0.1% trifluoroacetic acid (TFA). Their purity and liquid solubility were tested using LC-MS/MS, and 125 synthetic peptides were considered suitable for the current functional screening experiments. The peptide list contains those used in our previous study to search for bioactive factors that act on 3 types of vascular cells and affect in vivo mouse behavior when administered peripherally [5].

Cell Culture

The human monocytic leukemia cell line (THP1), rat fibroblast cell line (Rat-1), and UV♀2 cell line were obtained from the Riken Cell Bank (Ibaraki, Japan). Human aortic endothelial cells (HAoECs) and their associated culture media/supplements were purchased from PromoCell (Heidelberg, Germany). Rat pituitary tumor cells (GH_3), human uterine cervical carcinoma cells (HeLa), human umbilical vascular endothelial cells (HUEhT-1), human colorectal carcinoma cells (HCT116), human rhabdomyosarcoma cells (RD), and human embryonic kidney (HEK293) cells were purchased from the Japanese Collection of Research Bioresources Cell Bank (Osaka, Japan). Rat aortic smooth muscle cells (A-10) were obtained from American Type Culture Collection (USA). The cells were cultured in the appropriate medium with supplements as recommended by the suppliers. THP1 cells grown in RPMI1640 medium containing 10% fetal bovine serum were differentiated into macrophages by incubation with 500 ng/mL phorbol-12-myristate-13-acetate (PMA) (AdipoGen Life Sciences, Inc., San Diego, CA, USA) for more than 24 hours. Small interfering RNA (siRNA) duplexes against the human ATP synthase β-subunit (siATP5B) and scramble control siRNA were obtained from Santa Cruz Biotechnology (Dallas, TX, USA) and Bioneer Corporation (Oakland, CA, USA). THP1-derived macrophages cultured in 12-well dishes were incubated for 16 hours in Opti-MEM medium containing Lipofectamine RNAiMAX (Invitrogen, Carlsbad, CA, USA) with either 10 nM siATP5B or scramble control.

Determination of the Intracellular Free Ca^{2+} Concentration $[Ca^{2+}]_i$

Subconfluent THP1-derived macrophages grown in noncoated 96-well black plates with clear bottoms were deprived of serum for 16 hours and incubated with fluo-4-acetoxymethyl ester (Fluo 4-AM; Dojindo Molecular Technologies, Kumamoto, Japan) for 30 minutes at 37 °C in Hank's balanced salt solution (HBSS). Fluo 4-AM-loaded cells were washed 3 times with HBSS, treated with dissolved ANGT_HUMAN[448–462] peptide and read at an excitation wavelength of 485 nm and an emission wavelength of 535 nm using a Powerscan HT (BioTek Instruments Inc., Winooski, VT, USA) at the indicated times [8, 9]. RD, HUEhT-1, and HEK293 cells, in addition to Rat-1, HeLa, UV♀2, A-10, and GH3 cells, starved of serum for 2 hours were also tested for their ability to increase $[Ca^{2+}]_i$ in response to ANGT_HUMAN[448–462].

Real-Time Reverse Transcription–Polymerase Chain Reaction

Inhibition of endogenous ATP5B by siRNA was confirmed by quantifying the ATP5B mRNA levels. Total mRNA was isolated from THP1-derived macrophages using TRIzol reagent (Invitrogen, Carlsbad, CA, USA), reverse transcribed with a first-strand cDNA synthesis kit (Takara Bio, Shiga, Japan), and quantified using a CFX96 Touch Real-Time PCR Detection System (Bio-Rad Laboratories)-based reverse transcription–polymerase chain reaction (RT-PCR) protocol using KAPA SYBER (Nippon Genetics, Tokyo, Japan) as described previously [10]. Polymerase chain reaction primers for ATP5B (forward primer 5′-TGTCGATCTGCTAGCTCCCT-3′ and reverse primer 5′-CCTCTCACCAACACCAGCAA-3′) were synthesized by Eurofins Genomics (Tokyo, Japan).

Binding of Peptides to the Surfaces of Cultured Cells

THP1-derived macrophages and HeLa cells deprived of serum for 16 hours and growing HAoECs were incubated for 5 to 90 minutes after the addition of 10^{-6} M FAM-labeled ANGT_HUMAN[448–462]. Cells were washed 3 times with phosphate-buffered saline (PBS) and fixed with 4% paraformaldehyde for 15 minutes at room temperature. The nuclei were counterstained using DAPI Fluoromount-G (SouthernBiotech, Birmingham, AL, USA), and fluorescence signals were photographed using an LSM710 confocal

microscope (Carl Zeiss, Jena, Germany) as described previously [10, 11].

Retrieval of ANGT_HUMAN[448–462]-Bound Cellular Proteins

THP1 cells (8.8×10^6 cells) differentiated into macrophages were replaced with serum-free medium for 16 hours, washed twice with PBS, and then after the addition of 25 mM 4-(2-hydroxyethyl)-1-piperazineethanesulfonic acid (HEPES), the cells were scraped and centrifuged at 800*g* for 10 minutes at 4 °C. The supernatant was discarded, and the pellet was washed twice with 25 mM HEPES (pH 7.0) by centrifugation at 15 000*g* for 60 minutes at 4 °C. The pellet was then dissolved in Native PAGE sample buffer (Thermo Fisher Scientific, Waltham, MA, USA) containing 0.5% digitonin with or without either FAM-ANGT_HUMAN[448–462] or a fluorescent-labeled peptide of an unrelated sequence (GQGAHHAAGQAGNEAGR, SBSN_HUMAN[243–259]) (10^{-4} M) and incubated at room temperature for 30 minutes. The supernatant was collected after centrifugation at 20 000 × *g* for 30 minutes, and the protein concentration was quantified with a Nano Drop Lite UV-Vis spectrophotometer (Thermo Fisher Scientific), and 20 µg proteins/lane were subjected to clear-native polyacrylamide gel electrophoresis (CN-PAGE) using Native PAGE 4% to 16% Mini Protein Gel (Thermo Fisher Scientific) at 120 V for 120 minutes. Fluorescence was detected using a light-emitting diode (LED) illuminator. Native Mark Unstained Protein Standard (Thermo Fisher Scientific) was used as the molecular weight marker.

Extraction of ANGT_HUMAN[448–462]-Bound Cell Surface Proteins

THP-1-derived macrophages in 10-cm dishes (8.8×10^6 cells) were washed twice with PBS (pH 8.0) and incubated for 1 hour at 4 °C with 3.6 mL of 10^{-6} M biotinylated ANGT_HUMAN[448–462] dissolved in PBS. The cells were then overlaid for 30 minutes at room temperature with 5 mM bis (sulfosuccinimidyl) suberate (BS3) (Thermo Fisher Scientific), a cross-linking reagent. The cross-linking reaction was terminated by adding 20 mM Tris-HCl (pH 7.4) for 15 minutes at room temperature. The cells were scraped and centrifuged at 20 000*g* for 60 minutes at 4 °C. The pellet was dissolved in PBS, centrifuged at 20 000*g* for 60 minutes at 4 °C, resuspended in 300 µL radioimmunoprecipitation assay (RIPA) buffer (50 mM Tris-HCl, pH 7.6/150mM NaCl/1% NP-40/0.1% SDS), mixed for 10 minutes, sonicated for 10 minutes, rotated for 1 hour at 4 °C, and centrifuged again at 20 000*g* for 15 minutes at 4 °C to collect the supernatant. The biotinylated peptide-cell surface protein complexes in the solution were enriched and eluted using Dynabeads M280 streptavidin (Invitrogen, Carlsbad, CA, USA) as follows: 15 µL of Dynabeads-containing reagent was added to 1 mL PBS, vortexed for more than 30 seconds, and placed on the magnet for 1 minute to remove the PBS. The solution containing biotinylated peptide-cell surface protein complexes was added to Dynabeads, rotated for 30 minutes at room temperature, and placed onto the magnet to remove the supernatant. The beads in the tube were added to 300 µL RIPA buffer, mixed by inversion 100 times, and placed on a magnet to discard the supernatant. After repeating the washing procedure 6 times, biotinylated peptide-cell surface protein complexes adsorbed to Dynabeads were eluted by the addition of 60 µL 0.1% SDS for 5 minutes at 95 °C. Ten µL of the eluted sample per lane was loaded on a 10% to 20% gradient gel (DRC, Tokyo, Japan) at 200 V for 30 minutes using SDS Running Buffer (DRC) and transferred at 25 V for 30 minutes onto an Immune-Blot polyvinylidene fluoride (PVDF) membrane (Trans-Blot Turbo Mini PVDF Transfer Packs, Bio-Rad Laboratories, Hercules, CA, USA) using a Trans-Blot Turbo Transfer System. Precision Plus Protein Dual Color Standards (Bio-Rad Laboratories) were used as the molecular size markers. The PVDF membrane was blocked with Blocking One (Nacalai Tesque, Kyoto, Japan), washed 3 times with 2% bovine serum albumin/Tris-buffered saline containing 0.05% (w/v) Tween 20, and incubated at room temperature for 1 hour with peroxidase-conjugated anti-biotin IgG (1:10 000; Vector Laboratories Inc., Tokyo, Japan, RRID: AB_2336645), horseradish peroxidase (HRP)-labeled streptavidin (1:10 000; SeraCare, Milford, MA, USA), polyclonal anti-ANGT_HUMAN[448–462] IgG (1:1000, RRID: AB_2916121), or monoclonal anti-α-subunit (1:1000; Abcam, Cambridge, UK, RRID: AB_2801536) or anti-β-subunit of ATP synthase IgG (1:1000; Thermo Fisher Scientific, RRID: AB_221512). Bands were detected using Amersham ECL Prime Western Blotting Detection Reagent (GE Healthcare, Buckinghamshire, UK), photographed using ImageQuant LAS 4000 (GE Healthcare), and analyzed using ImageJ software.

Isolation of ANGT_HUMAN[448–462]-Binding Proteins in Rat Cerebrum Tissue

An 8-week-old female Jcl:Wistar rat (CLEA Japan, Tokyo, Japan) was deeply anesthetized with isoflurane, euthanized by decapitation, and the cerebrum was rapidly removed and homogenized on ice using a BL3000 homogenizer (Shinto Scientific Co., Tokyo, Japan) in 10 mL of 50 mM Tris-HCl buffer (pH 7.4) containing protease inhibitor cocktail (Nacalai Tesque Inc.). Homogenates were incubated with 0.5% digitonin (Thermo Fisher Scientific) for 4 hours at 4 °C and centrifuged at 20 000*g* for 60 minutes at 4 °C. The protein concentration of the supernatant was determined using a Nano Drop Lite UV-Vis spectrophotometer (Thermo Fisher Scientific). Aliquots of the supernatant were diluted with Native PAGE sample buffer (Thermo Fisher Scientific) to 2 µg/µL, incubated with 10^{-5} M FAM-ANGT_HUMAN[448–462] for 1 hour at 37 °C, and subjected to CN-PAGE on Native PAGE 4% to 16% mini protein gel (Thermo Fisher Scientific) and Native PAGE running buffer (Thermo Fisher Scientific) for 120 minutes at 120 V. The marker used was Native Mark Unstained Protein Standard (Thermo Fisher Scientific). Fluorescence was visualized using an LED illuminator and photographed, and fluorescent positive bands, together with negative gels of neighboring lanes at the same migration distance, were resected for in-gel trypsin digestion and subsequent LC-MS/MS analysis.

In-Gel Tryptic Digestion

Protein complexes separated by CN-PAGE were in-gel trypsin-digested using a previously described protocol [12, 13], but with the following modifications. Fluorescent protein spots showing the FAM-ANGT_HUMAN[448–462] complex in CN-PAGE were excised in rectangles of approximately 1 to 2 × 2 mm with a scalpel and washed with deionized water. The gel pieces were then dehydrated in 200 µL acetonitrile

for approximately 15 minutes and dried in an Iwaki VEC-100 micro-centrifugal vacuum concentrator (Asahi Techno Glass Co., Chiba, Japan) for 15 minutes. The proteins in the gel pieces were immersed in 100 μL of 10 mM DTT/25 mM ammonium bicarbonate for 1 hour at 56 °C, washed with 100 μL of 25 mM ammonium bicarbonate for 10 minutes, and incubated with 100 μL of 55 mM iodoacetamide in the dark at room temperature for 45 minutes. The pieces were washed with 25 mM ammonium bicarbonate for 10 minutes, dehydrated in 200 μL acetonitrile, dried in a centrifugal vacuum concentrator, and immersed in 20 μL of 50 mM Tris (pH 9.0) containing 100 ng/μL trypsin and 100 ng/μL Lys-C on ice for 45 minutes. Swollen gel pieces were placed in a minimal volume of 50 mM Tris (pH 9.0) for 24 hours at 37 °C, during which time peptide fragments digested in the gel pieces diffused into the surrounding solution. The solution was then transferred to siliconized plastic tubes on ice. Peptide fragments remaining in the gel pieces were further recovered after 20 minutes of incubation at room temperature in minimal volumes of 5% (v/v) formic acid containing 50% (v/v) acetonitrile. Peptide-containing solutions were pooled in siliconized tubes on ice. The combined solutions were desalted using stop-and-go extraction tips (stage tips) [14] filled with Empore C18 sealant (3M, Saint Paul, MN, USA), prewashed with 50 μL of methanol, equilibrated with 50 μL of 70% acetonitrile containing 0.1% TFA, and then washed with 80 μL of 0.1% TFA. The peptides were eluted with 80 μL 50% acetonitrile containing 0.1% TFA. The sample solutions were then lyophilized and redissolved in 20 μL of 3% acetonitrile containing 0.1% formic acid for LC-MS/MS analysis.

LC-MS/MS Analysis of Peptide-Bound Proteins

An ultra-sensitive LC-MS system combining LC (Easy-n LC 1000, Thermo Fisher Scientific) and Q-Exactive (Thermo Fisher Scientific) was used, as previously described [15]. Database searches were performed using the SEQUEST algorithm [16] incorporated into Proteome Discoverer 1.4.0.288 software (Thermo Fisher Scientific). The search parameters were as follows: enzyme, trypsin; variable modification, oxidation of Met residue; variable modification, carbamidomethylation of Cys residue; peptide ion mass tolerance, 6 ppm; and fragment ion mass tolerance, 0.02 Da, which were searched for in the decoy database and the FDR was set as 0.01, using Percolator scoring with posterior error probability (PEP) validation. Peptide quantitation was performed using Proteome Discoverer 1.4.0.288. The detected proteins classified into membrane, receptor, or transport categories using the DAVID bioinformatics database were selected, and their peptide spectrum match (PSM) levels were evaluated.

Production and Purification of ANGT_HUMAN[448–462] Antibody

The specific polyclonal antibody against ANGT_HUMAN[448–462] (RRID: AB_2916121) was raised and purified as described previously [12, 17], with the following modifications. Two micrograms of [Cys^0]-KPEVLEVTLNRPFLF were chemically synthesized, and approximately half was pretreated with a protein cross-linking and fixation reagent, mixed with the remaining 1 μg of untreated peptide, coupled to maleimide-activated mariculture keyhole limpet hemocyanin (Pierce), and immunized on days 1, 15, 29, 43, and 57 into Japanese white rabbits in the laboratory of Scrum Inc (Tokyo, Japan). Blood was collected prior to the first injection and on days 36, 50, and 64 post-injection. The antibody titer was determined using enzyme-linked immunosorbent assay. The polyclonal antisera showing the highest titer were purified using a Melon Gel IgG Spin Purification Kit (Thermo Fisher Scientific), which removed nonrelevant proteins that are often present in high abundance. The purified antibody did not recognize angiotensin II or other angiotensinogen-derived synthetic peptides.

Immunohistochemical and Immunofluorescent Staining

A human healthy tissue microarray, MNO341 (US Biomax, Rockville, MD, USA), which contained biospecimens of 33 tissue types mostly from surgical resections, and a normal brain tissue microarray, BNC17011a (US Biomax, Rockville, MD, USA), which contained 80 cores from 25 cases, were used to examine the tissue distribution of ANGT_HUMAN[448–462] peptide. Tissue preparations were deparaffinized, rehydrated, and autoclaved in citric acid buffer (pH 6.0) for antigen retrieval.

For immunohistochemistry, MNO341 preparations were blocked using an Avidin biotin blocking kit (Nichirei Bioscience, Tokyo, Japan) and incubated overnight at 4 °C with either anti-ANGT_HUMAN[448–462] IgG (RRID: AB_2916121) or control nonimmune IgG purified from preimmune serum (1:1000 dilution). The sections were washed 3 times with PBS and incubated with a goat anti-rabbit IgG HRP conjugate (1:3000, Bio-Rad, RRID: AB_11125142) for 60 minutes at room temperature. Antibody binding was visualized using the avidin-biotin-complex peroxidase method with a Vectastain ABC kit (Vector Laboratories Inc.), including diaminobenzidine tetrahydrochloride (Nacalai Tesque). Tissue preparations were stained with hematoxylin (Muto Pure Chemicals, Tokyo, Japan).

For dual immunofluorescence staining to detect the cellular co-localization of angiotensin II and ANGT_HUMAN[448–462] in human tissues, MNO341 and BNC17011a preparations were blocked using Blocking One (Nacalai Tesque Inc.) and then incubated simultaneously with 2 primary antibodies, rabbit anti-ANGT_HUMAN[448–462] IgG (1:1000, RRID: AB_2916121) and mouse anti-human angiotensin II/III (1:500, Novus Biologicals, Centennial, CO, USA, RRID: AB_959119), at room temperature for 90 minutes. The sections were washed 3 times with PBS and incubated with goat anti-rabbit-Alexa Fluor 488-conjugated antibody (1:1000, Abcam, RRID: AB_2630356) and goat anti-mouse-Alexa Fluor 594-conjugated antibody (1:1000, Thermo Fischer Scientific, RRID: AB_2534073). The nuclei were counterstained using DAPI Fluoromount-G (SouthernBiotech, Birmingham, AL, USA) and images were acquired using an LSM710 confocal microscope (Carl Zeiss).

Co-localization of Immunoreactive ATP Synthase and Cell Surface-Bound ANGT_HUMAN[448–462]

THP1 cells plated and differentiated into macrophages on glass coverslips in a 12-well plate (Watson Bio Lab, Tokyo, Japan) were pretreated for 30 minutes with or without 10^{-5} M β-casomorphin 7 (Peptide Institute, Osaka, Japan), an antagonist of the β-subunit of ATP synthase [11, 18], and incubated with 10^{-6} M FAM-ANGT_HUMAN[448–462] for 60 minutes. Cells were then washed 3 times with PBS, blocked with

Blocking One (Nacalai Tesque Inc.) for 30 minutes, fixed with 4% paraformaldehyde for 15 minutes, and incubated for 60 minutes with either anti-α-subunit ATP synthase antibody (1:1000, Abcam, RRID: AB_2801536) or anti-β-subunit ATP synthase antibody (1:1000, Thermo Fisher Scientific, RRID: AB_221512). The immunoreactive α-subunit and β-subunit of ATP synthase were visualized after 30-minute incubation with Alexa Fluor 594 goat anti-rabbit IgG[H + L] (1:3000, Abcam, RRID: AB_2650602) and anti-mouse IgG[H + L] (1:3000, Life Technologies, RRID: AB_2534073), respectively. Nuclei were counterstained using DAPI Fluoromount-G (SouthernBiotech, Birmingham, AL, USA). Laser scanning confocal microscopy was performed using an LSM710 confocal microscope (Carl Zeiss, Oberkochen, Germany).

Measurements of Plasma ANGT_HUMAN[448–462] Levels

The stable isotope-labeled ANGT_HUMAN[448–462] peptide was synthesized by Scrum Inc. using L-phenylalanine-N-9-fluorenylmethoxycarbonyl ($^{13}C_9$, 98%; ^{15}N, 98%): KPEVLEVTLNRPELF, with the underlined residue containing a stable isotope. This peptide was spiked into 50 µL human plasma at a final concentration of 2 nM and enriched using a modified differential solubilization protocol, as described previously [3]. The obtained low-molecular-weight peptide fractions extracted from 800 µL of human plasma were lyophilized and redissolved in LC-MS/MS-compatible surfactants and separated by reverse-phase (RP)-HPLC, collected at 1-minute intervals and combined into 8 fractions by the cyclic sample pooling method [5, 19]. The extracts derived from 80 µL of plasma were analyzed using a quadrupole Orbitrap benchtop mass spectrometer, Q-Exactive (Thermo Fisher Scientific), equipped with an EASY-nLC 1000 system (Thermo Fisher Scientific) essentially as described previously [20]. The peptides were injected directly onto an analytical column (C18, particle diameter 3 µm, 75 µm i.d. × 125 mm, Nano HPLC capillary column, Nikkyo Technos, Tokyo, Japan) and separated using a gradient composed of solvent A (0.1% formic acid) and solvent B (0.1% formic acid and 90% acetonitrile) (0-2 minutes, 0% to 10% B; 2-20 minutes, 10% to 30% B; 20-25 minutes, 30% to 55% B; 25-27 minutes, 80% B) at a flow rate of 300 nL/min. MS spectra were collected over an m/z range of 350 to 650 at a resolution of 70 000 at 200 m/z to set an automatic gain control (AGC) target of 3×10^6. The 5 most intense ions with charge states of 2 + to 6 + that exceeded an intensity of 4×10^4 were fragmented in a data-dependent mode via collision-induced dissociation with a normalized collision energy of 27%. Tandem mass spectra were acquired using an Orbitrap mass analyzer with a mass resolution of 70 000 at 200 m/z to set an AGC target of 5×10^5. The dynamic exclusion time was set at 30 seconds. Plasma concentrations were extrapolated from the extracted ion chromatograms (XICs) generated using the respective endogenous peptides and the corresponding spiked, stable isotope-labeled peptides [20-22].

In Vivo Analysis of Water/Food Intake and Spontaneous Locomotor Activity

Adult male C57BL/6J mice weighing 25 to 30 g (CLEA Japan) were maintained as described previously [5, 23] in a controlled temperature environment (22-25 °C), with a 12-hour light-dark cycle (lights on 08:00 hours to 20:00 hours), with free access to food (standard laboratory chow; CE2, CLEA Japan) and water. After at least 7 days of habituation with saline injections on weekdays, the mice were intraperitoneally injected with the indicated doses of synthetic peptides dissolved in 100 µL double-distilled water (ddH_2O) or with 100 µL ddH_2O alone using a 27G needle without anesthesia approximately 10 to 40 minutes before the start of the dark period.

For intracerebroventricular injection of peptides, mice were anesthetized and stereotaxically implanted with a stainless-steel guide cannula in the lateral ventricle, as previously described [24, 25]. The mice underwent more than 1 week of postoperative recovery and were injected manually with 1 µL of 0.1% TFA saline solution alone or with 1.0, 10, 100, or 1000 fmol synthetic peptides over 1 minute via the indwelling cannula without anesthesia approximately 10 to 40 minutes before the start of the dark period.

Food and water intake and locomotor activity were recorded using a simultaneous monitoring system (ACTIMO-100M combined with MFD-100; Shinfactory, Fukuoka, Japan), as previously described [5, 24, 25]. The monitoring system was equipped with beam sensors located every 2 cm along the floor of the cage enclosure, and the ACTIMO-DATA software (Shinfactory) detected animal movement by continuously counting interruptions of the infrared photobeam emitted every 0.5 second. To eliminate any artifacts elicited by respiration or nose/tail movements, the simultaneous interruption of more than 2 neighboring beams was recorded as "an activity output" by the ACTIMO-DATA software (Shinfactory). Movement signal counts were imported in real-time using the Spike2 analysis program (Cambridge Electronic Design, Cambridge, UK). A food container was designed to prevent mice from dragging food into their bedding and to avoid spillover, and the minimum quantity of measurable food using the microbalance was 0.01 g. Water intake was measured using a drop counting system. Food and water intakes were recorded simultaneously every 3 minutes. The experiments were performed during the dark phase in a room that was completely isolated from external noise.

Statistical Analysis

Data are presented as mean ± standard error of the mean (SEM) and were analyzed using GraphPad Prism software 5.02 (GraphPad Software Inc., San Diego, CA, USA). Mouse behavioral experimental data involving 3 or more groups were analyzed using 2-way analysis of variance (ANOVA) followed by Tukey–Kramer's post hoc test. Statistical significance was set at $P < 0.05$.

Ethics Approval and Consent to Participate

All animal experimental procedures were approved by the Animal Experimentation and Ethics Committee of Kitasato University School of Medicine (2016-144). The procedures were performed in compliance with the ARRIVE guidelines and with the guidelines for animal experiments at the Kitasato University School of Medicine. All the study methods were performed in accordance with the relevant guidelines and regulations of this organization as well as the Ethical Guidelines for Medical and Health Research Involving Human Subjects in Japan. The study protocol for human blood samples was approved by the Ethics Committee of Kitasato University Hospital/School of Medicine (C19-245).

Results

Functional Screening of Synthetic Peptides Using Cultured Cells

Our plasma peptidomics analysis and subsequent de novo sequencing-based database search confirmed the presence of 7959 distinct plasma native peptides with peptide identification false discovery rates (FDRs) of 0% [5]. We selected peptide sequences *in silico* for subsequent functional screening studies, chemically synthesized the sequences, and consecutively tested their purity and liquid solubility using LC-MS/MS. As a result, 129 synthetic peptides were judged appropriate for biological validation experiments. Many of these peptides were used in our previous screening study to test their biological activities in vascular cells and in vivo experiments, which led to the discovery of 3 suprabasin-derived peptides (SBSN_HUMAN[225-237], SBSN_HUMAN[243-259], and SBSN_HUMAN[279-295]) [5] and a proGIP-derived peptide (GIP_HUMAN[22-51]) [20]. The biological activities of the remaining 125 peptides were screened using a variety of mammalian cells in culture, and experiments were performed to examine their ability to induce the expression of genes downstream of major intracellular signaling molecules, to increase $[Ca^{2+}]_i$, and to induce mitogenesis.

A 15-amino-acid residue peptide derived from angiotensinogen, KPEVLEVTLNRPFLF, designated ANGT_HUMAN[448–462] (Fig. 1a and 1b), induced an increase in $[Ca^{2+}]_i$ in THP1-derived macrophages and a rat fibroblast cell line, Rat-1. The ability of ANGT_HUMAN[448–462] to elicit an increase in $[Ca^{2+}]_i$ was detected only at rather high concentrations (10^{-6} to 10^{-5} M) (Fig. 2a) and was not observed in the murine- and human-derived vascular, endocrine, and epithelial cell lines: A10, HUEhT-1, HeLa, HEK293, RD, UV♀2, and GH_3. Our strenuous efforts to search for any genes stimulated by the addition of ANGT_HUMAN[448–462] (10^{-9} to 10^{-7} M) in cultured human, rat, and mouse-derived cells were unsuccessful. Pretreatment of THP1-derived macrophages with the dihydropyridine-sensitive calcium channel antagonist nicardipine blocked the ANGT_HUMAN[448–462]-induced $[Ca^{2+}]_i$ response (Fig. 2a). These results suggest that ANGT_HUMAN[448–462] causes extracellular calcium influx into THP1-derived macrophages via the ATP synthase β-subunit. To confirm that ANGT_HUMAN[448–462] binds to the intact cell surface, we overlaid growing cells in culture with the peptide labeled with 5-carboxyfluorescein at the N-terminus (FAM-ANGT_HUMAN[448–462]) and observed them with confocal immunofluorescence microscopy after extensive washing. The addition of FAM-ANGT_HUMAN[448–462] (10^{-6} M) clearly increased the immunofluorescence signal intensity on the surfaces of THP1-derived macrophages, HAoECs, and HeLa cells in 5 to 90 minutes (Fig. 2b-2d), but negligible fluorescence binding was detected in other cell lines tested. Despite the large ANGT_HUMAN[448–462] dose required to induce $[Ca^{2+}]_i$ in THP1 cells and the absent $[Ca^{2+}]_i$ upregulation in HeLa cells, FAM-ANGT_HUMAN[448–462] peptide apparently bound to THP1-derived macrophages, HAoECs, and HeLa cells. We speculated that the major biological effects of ANGT_HUMAN[448–462] might not be mediated by increased $[Ca^{2+}]_i$ or the induction of gene expression. Therefore, we designed a study to explore cell surface binding proteins/receptors using THP1-derived macrophages that showed the most abundant cell-surface binding and cell responses to the peptide.

Retrieval of Cell Membrane Proteins Binding With ANGT_HUMAN[448–462]

Next, we searched for cell membrane proteins that bind to ANGT_HUMAN[448–462] using a far simpler protocol than the method we previously used to identify salusin-β receptors using membrane protein-embedded artificial liposomes [11]. Cell protein fractions prepared from THP1-derived macrophages were incubated with FAM-ANGT_HUMAN[448–462], and after extensive washing, they were subjected to CN-PAGE, which maintains peptide-protein complexes during electrophoresis. The fluorescent band was faint but was visualized at the migration distance of a molecular size marker clearly distinct from the unbound fluorescent peptide (Fig. 2e, lanes 3-6). Protein samples extracted from THP1-induced macrophages treated with fluorescently labeled peptides of unrelated sequences, such as FAM-SBSN_HUMAN[243-259] (GQGAHHAAGQAGNEAGR), did not show any visible fluorescent signal on the gels (Fig. 2e, lanes 7-10). The fluorescence-positive bands, in addition to the corresponding invisible gel positions of the neighboring lanes where control cell lysates without fluorescent peptides were loaded (Fig. 2e, lanes 1 and 2), were in-gel trypsin-digested and analyzed using LC-MS/MS. Among the detected proteins classified as membrane, receptor, or transport categories using the DAVID bioinformatics database, the following 3 showed distinctly high PSMs in the in-gel digests derived from FAM-ANGT_HUMAN[448–462]-treated cells compared with those from cells in the negative control experiments: α-subunit of ATP synthase, mitochondrial (ATP5A), β-subunit of ATP synthase (ATP5B), and plasminogen activator urokinase receptor (PLAUR). The PEP scores [26] of the identified peptides revealed high validity estimates for these identifications (Table 1).

Next, we studied whether the β-subunit of ATP synthase that co-migrated with FAM-ANGT_HUMAN[448–462] could also be retrieved from cell-surface proteins, because ATP synthase is abundantly expressed in intracellular mitochondrial membranes [27, 28] as well as on the surfaces of many cell types [29-35]. We overlaid biotinylated ANGT_HUMAN[448–462] peptide onto the culture media of growing THP1-derived macrophages, after which the ANGT_HUMAN[448–462] peptide bound to the cell surface proteins was treated with bis (sulfosuccinimidyl) suberate. The cells were harvested, and cell lysates were incubated for 30 minutes with streptavidin-coated magnetic beads and eluted in 0.1% SDS at 95 °C. This procedure retrieved biotinylated peptide-protein complexes and endogenous biotin-binding proteins in the eluates, which were then electrophoresed using SDS-PAGE and immunoblotted. Horseradish peroxidase (HRP)-conjugated anti-biotin generated a distinct band of approximately 15 kDa in biotinylated ANGT_HUMAN[448–462]-treated cells (Fig. 2f, lane 1), whereas in untreated control cells, an endogenous biotin-binding protein of approximately 75 kDa was detected (Fig. 2f, lanes 2 and 3). HRP-conjugated streptavidin similarly visualized a 15-kDa protein band in cell lysates derived from THP1 cells overlaid with and cross-linked to ANGT_HUMAN[448–462], but not in those untreated with the peptide (Fig. 2g). Immunoblotting using polyclonal anti-ANGT_HUMAN[448–462] detected the same 15-kDa protein band in ANGT_HUMAN[448–462]-treated and cross-linked cell-derived proteins (Fig. 2h). To confirm the migration of ANGT_HUMAN[448–462] with

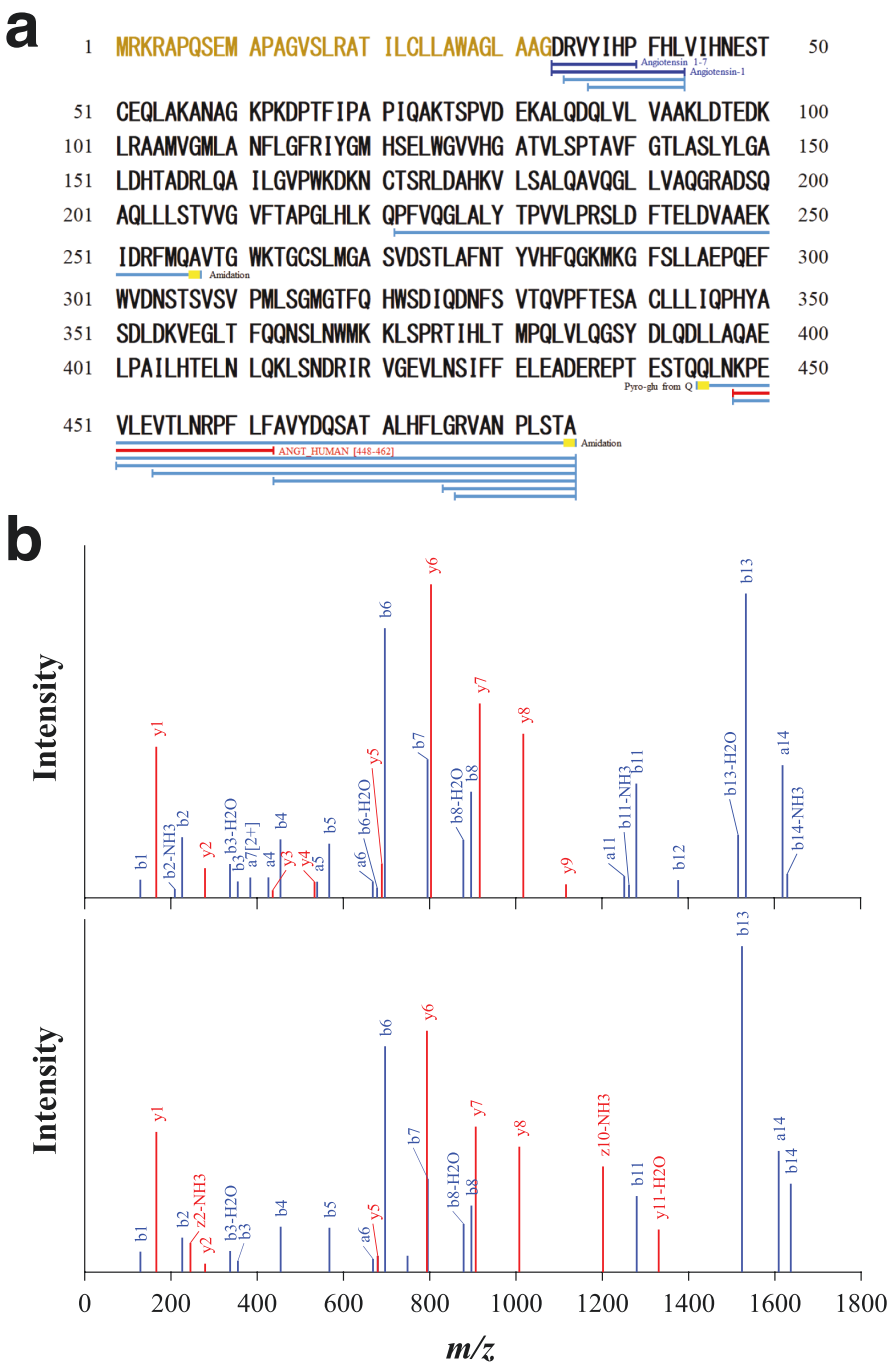

Figure 1. Peptidomic identification of ANGT_HUMAN[448–462] from human plasma. (a) Sequence alignment of ANGT_HUMAN[448–462] (red horizontal line) and other cleaved products of proangiotensinogen identified with an FDR of 0% (blue horizontal lines) using peptidomic analysis. The predicted signal peptide of the preproprotein is shown in yellow letters and authentic angiotensin [1-7] and angiotensin I peptides are shown in dark blue lines. Yellow squares denote the amino acid undergoing modification. (b) Annotated MS/MS fragmentation spectra for plasma ANGT_HUMAN[448–462] filtered using peptidomic analysis and comparisons with those of the corresponding synthetic ANGT_HUMAN[448–462] peptides. MS/MS spectra with sequence assignments of fragment ions corresponding to synthetic ANGT_HUMAN[448–462] "KPEVLEVTLNRPFLF" with an *m/z* 530.9565 ($z = 6$; upper panel) are compared with those of endogenous peptides (lower panel) to confirm the putative identification. MS/MS spectra were deconvoluted into singly charged ions from the observed spectra and peaks were assigned theoretical *m/z* values for fragment ions. The annotations of the identified matched N-terminal-containing ions are shown in blue and the C-terminal-containing ions in red. The *m/z* differences between theoretical and observed values for most assigned peaks were less than 0.01 Da.

the α- and β-subunits of ATP synthase, the same protein samples were immunoblotted using specific antibodies against the α- and β-subunits of ATP synthase. Immunoreactivity was detected at 15 kDa in both ANGT_HUMAN[448–462]-treated and nontreated cell-derived proteins, confirming the migration of ANGT_HUMAN[448–462] and α- and β-subunits of ATP synthase (Fig. 2i and 2j).

Cell surface ATP synthase is known to mediate important biological activities, such as angiogenesis [11, 34, 35] and lipid accumulation [29], as well as suppression of food intake

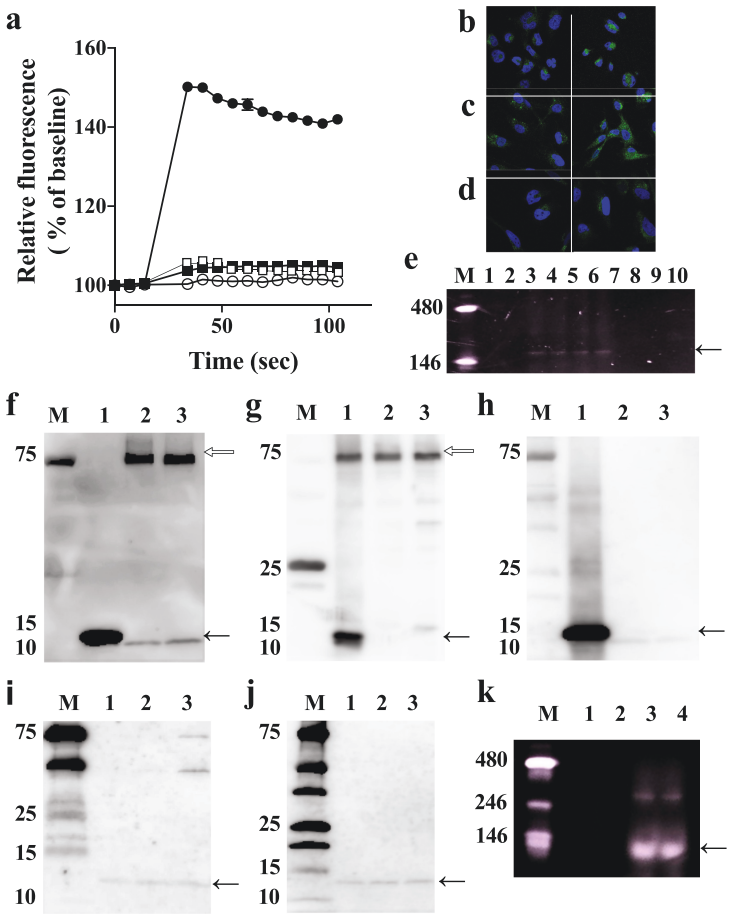

Figure 2. Binding of ANGT_HUMAN[448–462] to cultured cells. (a) Effect of ANGT_HUMAN[448–462] on $[Ca^{2+}]_i$ in THP1-derived macrophages. Cells were stimulated with ANGT_HUMAN[448–462] (closed circle: 10^{-5} M, closed square: 10^{-6} M, open circle: control) and Fluo-4/AM fluorescence intensities were monitored. Cells pretreated with 10^{-5} M nicardipine were stimulated with 10^{-5} M ANGT_HUMAN[448–462] (open square). Points with bars represent mean ± SD (n = 6). (b–d) Confocal laser-scanning microscopy images of fluorescent ANGT_HUMAN[448–462] peptide bound to cultured cells. Growing THP1-derived macrophages (b), HAoECs (c), or HeLa cells (d) were overlaid without (left panels) or with 10^{-6} M ANGT_HUMAN[448–462] (right panels), nuclei counterstained with DAPI (blue), and the cell surface-bound green fluorescence photographed. (e) Total cell proteins extracted from THP1-derived macrophages were incubated without (lanes 1, 2) or with 10^{-4} M FAM-ANGT_HUMAN[448–462] (lanes 3-6) or unrelated fluorescent-labeled peptide (lanes 7-10) and loaded on CN-PAGE and fluorescence detected. An arrow indicates the position of visualized fluorescent bands in lanes 3 to 6. Lane M: Native Mark unstained protein standards. (f-j) THP1-derived macrophages were overlaid with (lane 1) or without (lanes 2 and 3) 10^{-6} M biotinylated ANGT_HUMAN[448–462] and, after incubation with (lanes 1 and 2) or without (lane 3) a cross-linking reagent, biotinylated peptide-bound plasma membrane protein complexes were extracted using streptavidin-coated magnetic beads and immunoblotted using peroxidase conjugated anti-biotin (f), peroxidase-conjugated streptavidin (g), anti-ANGT_HUMAN[448–462] IgG (h), anti-α-subunit of ATP synthase IgG (i) or anti-β-subunit of ATP synthase IgG (j). Arrow indicates the position of immunoreactive positive bands. An open arrow denotes the position of endogenous biotin-bound proteins. Lane M, molecular weight marker. (k) Rat cerebrum tissue lysates were solubilized, incubated without (lanes 1 and 2) or with (lanes 3 and 4) 10^{-5} M FAM-ANGT_HUMAN[448–462] and subjected to CN-PAGE. Lane M, Native Mark unstained protein standards. An arrow indicates the position of fluorescent bands detected in FAM-ANGT_HUMAN[448–462]-treated tissue proteins.

[25, 36-39] elicited by chemicals [18, 29], digested products [37-39], and endogenous proteins [25, 34, 35]. Therefore, we next studied whether ATP synthase subunits can also be retrieved from brain tissues that contain satiation and appetite centers, using the same strategy as described above. Aliquots of homogenized rat cerebral tissue were incubated with or without FAM-ANGT_HUMAN[448–462] and separated using CN-PAGE. Clear fluorescent peptide-protein complex bands were detected, resected, and in-gel trypsin-digested for subsequent LC-MS/MS analysis (Fig. 2k). The fluorescent protein bands contained the β-subunit of ATP synthase (ATP5B) with far greater PSM values than those of invisible bands in neighboring lanes loaded with control samples untreated with FAM-ANGT_HUMAN[448–462]. The PEP scores of the 9 identified digests indicated high validity estimates (Table 2). These results confirmed that ATP synthase proteins are expressed on the surface of THP1-derived macrophages and in rat brain tissues and bound to and migrated with ANGT_HUMAN[448–462].

ATP Synthase as a Cell Surface Protein Binding With ANGT_HUMAN[448–462]

Using specific monoclonal antibodies against the α- and β-subunits of ATP synthase, we performed immunofluorescence staining of THP1-derived macrophages that had been pretreated with FAM-ANGT_HUMAN[448–462] to demonstrate whether the bound fluorescent peptides were co-localized with the ATP synthase expressed on the cells (**Fig. 3**). Confocal laser scanning microscopy revealed that specific cell surface fluorescent signals by

Table 1. Proteins classified under membrane, receptor, or transport categories identified by LC-MS/MS analysis of in-gel trypsin-digests of a fluorescent peptide-protein complex band (Fig. 2e, lanes 3-6)

Protein name	UniProt accession	Gene name	Peptide sequence	MH+	PEP	Charge	m/z
β-subunit of ATP synthase[a]	P06576	ATP5B[b]	LVLEVAQHLGESTVR	1650.91770	0.009166	3	550.97742
			IGLFGGAGVGK	975.5623	0.007526	2	488.2848
			VVDLLAPYAK	1088.63494	0.002025	2	544.81995
			FTQAGSEVSALLGR	1435.7533	0.001876	2	718.3803
			IMDPNIVGSEHYDVAR	1815.86789	0.00007986	3	605.96075
Urokinase plasminogen activator surface receptor	Q03405	PLAUR	GPMNQC*LVATGTHEPK	1739.82071	0.00007273	3	580.61243
			SGC*NHPDLDVQYR	1560.68479	0.009478	3	520.89978
α-subunit of ATP synthase[c]	P25705	ATP5A[d]	VVDALGNAIDGK	1171.63127	0.0501	2	586.31927

Each peptide was identified with a false discovery rate of 1%. Abbreviations: C*, cystine residue with modification of carbamidomethyl; PEP, posterior error probabilities.
[a]The protein name registered in the UniProt database is ATP synthase F1 subunit beta or ATP synthase subunit beta, mitochondrial.
[b]The gene names registered in the UniProt database are ATP5B, ATP5F1B, ATPMB, or ATPSB.
[c]The protein name registered in the UniProt database is ATP synthase F1 subunit alpha or ATP synthase subunit alpha, mitochondrial.
[d]The gene names registered in the UniProt database are ATP5A, ATP5A1, ATP5F1A, ATP5AL2, or ATPM.

Table 2. Tryptic peptides detected by LC-MS/MS analysis of in-gel trypsin-digests of a fluorescent peptide-protein complex band (Fig. 2k)

Protein name	UniProt accession	Gene name	Sequence	MH+	PEP	Charge	m/z
β-subunit of ATP synthase[a]	P10719	Atp5b[b]	LVLEVAQHLGESTVR	1650.92044	9.164E-07	3	550.97833
			IPVGPETLGR	1038.59465	0.00796	2	519.80096
			IGLFGGAGVGK	975.56249	0.0002068	2	488.28387
			TVLIMELINNVAK	1457.84001	0.00003735	2	729.42365
			VALVYGQMNEPPGAR	1601.81450	0.01388	2	801.41089
			VALTGLTVAEYFR	1439.79094	2.572E-08	2	720.39929
			FTQAGSEVSALLGR	1435.75481	5.318E-07	2	718.38104
			IMDPNIVGSEHYDVAR	1815.87174	0.00001868	3	605.95959
			IM*DPNIVGSEHYDVAR	1831.86399	0.006308	3	611.29211

Each peptide was identified with a false discovery rate of 1%. Abbreviations: M*, oxidized methionine residue; PEP, posterior error probabilities.
[a]The protein name registered in the UniProt database is ATP synthase F1 subunit beta or ATP synthase subunit beta, mitochondrial.
[b]The gene name registered in the UniProt database is Atp5f1b or Atp5b.

FAM-ANGT_HUMAN[448–462] co-localized very well with the immunoreactive ATP synthase β-subunit and less strongly with the α-subunit (Fig. 3a and 3b). The binding of FAM-ANGT_HUMAN[448–462] to the cells was significantly inhibited by pretreatment of the cells with excess β-casomorphin 7, an antagonist of anorectic peptides that acts on the cell surface ATP synthase [37, 40] (Fig. 3c and 3d). The α- and β-subunit ATP synthase-like immunoreactivity on immunohistochemistry was also reduced by pretreating the cells with excess β-casomorphin 7 before incubating them with their respective antibodies (Fig. 3c and 3d). Transfection of ATP synthase β-subunit siRNA (siATP5B) into THP1-derived macrophages markedly attenuated the immunoreactive ATP synthase β-subunit and decreased the fluorescent signals on the cell surface elicited by ANGT_HUMAN[448–462], whereas scramble control siRNA had no effect (Fig. 3e and 3f). Pretreatment of cells with anti-ATP synthase β-subunit antibody inhibited the fluorescent signals elicited by FAM-ANGT_HUMAN[448–462], whereas the effect of the anti-ATP synthase α-subunit antibody was limited (Fig. 3g and 3h). Taken together, these results demonstrate that ANGT_HUMAN[448–462] binds to the cell surface where the β-subunit of ATP synthase is expressed.

Presence of ANGT_HUMAN[448–462] in Human Organs, Cells, and Plasma

We investigated the systemic expression of ANGT_HUMAN[448–462] by staining a healthy human tissue microarray with a specific polyclonal antibody raised against ANGT_HUMAN[448–462]. Immunohistochemistry using IgG purified from the preimmune rabbit serum did not detect any significant signals. In contrast, immunoreactive ANGT_HUMAN[448–462] was abundantly detected in major human organs, such as the stomach, liver, colon, thyroid, and kidney, and was significantly less abundant in the cerebral cortex, pituitary, spinal cord, lungs, and heart (Fig. 4a-4j). We next searched for cultured human cells that expressed ANGT_HUMAN[448–462]-like immunoreactivity. Confocal immunofluorescence microscopy revealed the expression of THP1-derived macrophages, HAoECs, RD, HCT116, HeLa, and HUEhT-1 cells (Fig. 5a-5f).

Since ANGT_HUMAN[448–462] is an endogenously processed product of proangiotensinogen, a well-known precursor of angiotensin II, we investigated whether ANGT_HUMAN[448–462] and angiotensin II co-localized within cells by co-staining the 2 peptides. Confocal laser scanning microscopy of immunofluorescent double-staining revealed co-localization of the 2 peptides in the cells of several

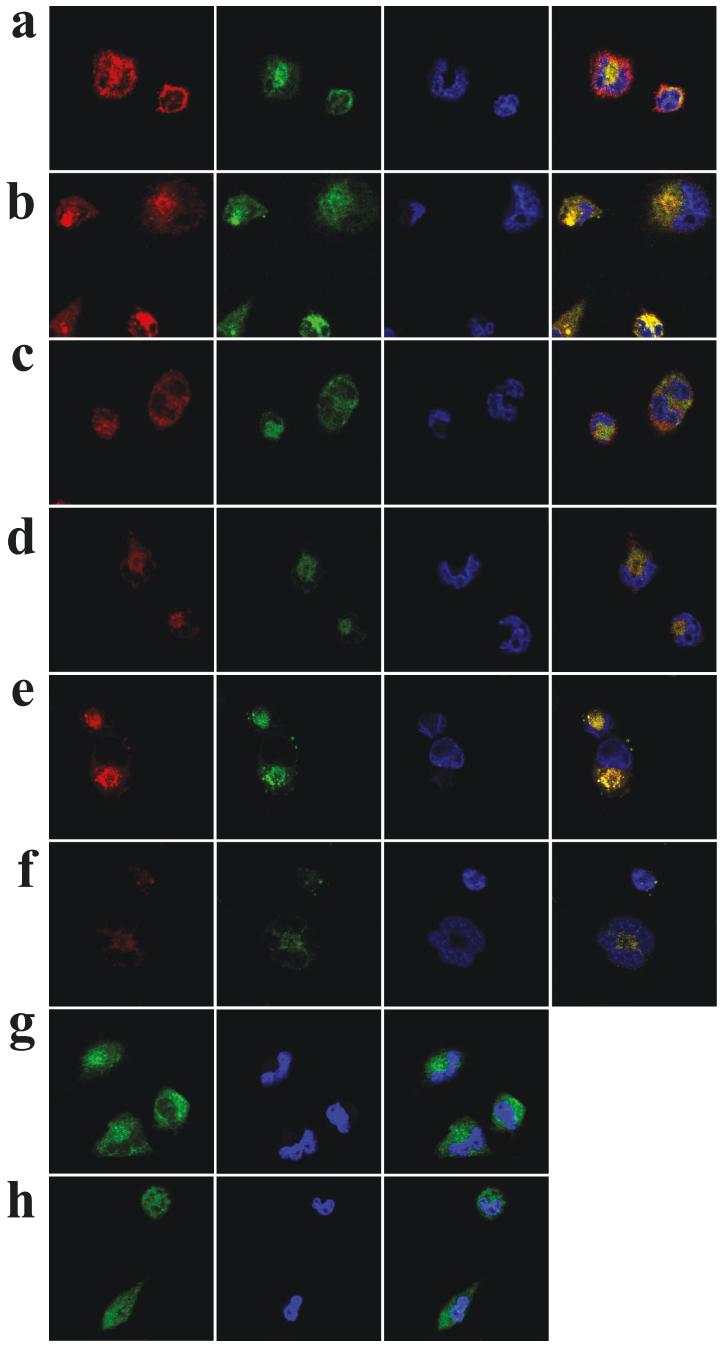

Figure 3. Fluorescent ANGT_HUMAN[448–462] binding to the THP1 cell surface and its immunofluorescence co-localization with the α- and β-subunits of ATP synthase. (a–d) FAM-ANGT_HUMAN[448–462] (10^{-6} M) was overlaid for 60 minutes on THP1-derived macrophages pre-treated without (a, b) or with 10^{-5} M β-casomorphin 7 (c, d) for 30 minutes and fixed and stained with the ATP synthase α-subunit antibody (a, c) or β-subunit antibody (b, d) (1:1000). (e, f) THP1-derived macrophages, transfected with either scramble control siRNA (e) or siATP5B (f), were incubated with FAM-ANGT_HUMAN[448–462] (10^{-6} M) for 60 minutes and stained with ATP synthase β-subunit antibody (1:1000). (g, h) THP1-derived macrophages, serum-starved for 16 hours and pretreated for 60 minutes with antibody against the ATP synthase α-subunit (1:1000) (g) or β-subunit (1:1000) (h), were incubated with FAM-ANGT_HUMAN[448–462] (10^{-6} M) for 60 minutes. The green signals correspond to FAM-ANGT_HUMAN[448–462] peptide bound to the cell surface, while the red signals represent the localization of immunoreactivity of the α- and β-subunit of ATP synthase visualized using Alexa Fluor goat anti-rabbit IgG[H + L] and anti-mouse IgG[H + L] (1:3000), respectively. The nuclei were counterstained with DAPI (blue). Overlay resulted in yellow signals indicative of co-localization.

organs, such as the cerebral cortex, medulla oblongata, pituitary gland, midbrain, pons, lung, heart, colon, stomach, and renal tubules (Fig. 6a-6j). In contrast, distinct localizations were clearly detected in tissues such as the renal glomeruli and thyroid gland (Fig. 7a-7a‴ and 7b-7b‴). In the liver, angiotensin II-like immunoreactivity was overwhelmingly abundant, whereas ANGT_HUMAN[448–462] was only faintly stained when stained simultaneously (Fig. 7c–7c‴). The wide distribution of immunoreactive ANGT_HUMAN[448–462] in human tissues concurs with the known angiotensinogen gene expression profile, suggesting that the translated angiotensinogen transcripts may

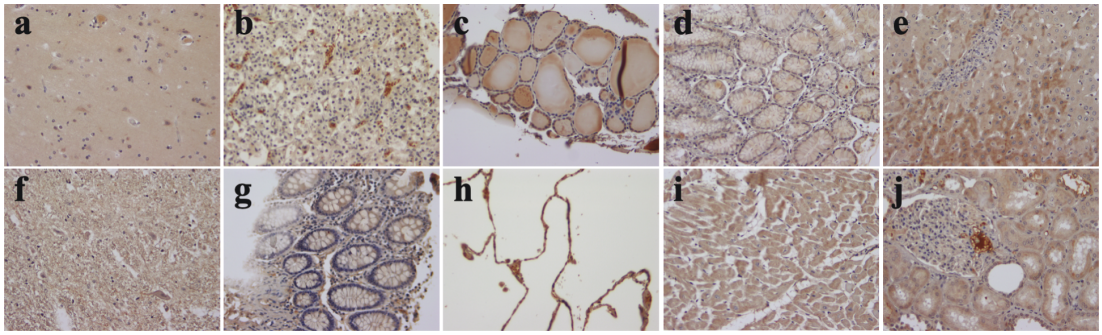

Figure 4. Systemic distribution of ANGT_HUMAN[448–462]-like immunoreactivity in human organs. Human tissue array sections were immunohistochemically stained with anti-ANGT_HUMAN[448–462] at 1:1000 dilution. (**a**) cerebral cortex, (**b**) pituitary gland, (**c**) thyroid, (**d**) stomach, (**e**) liver, (**f**) spinal cord, (**g**) colon, (**h**) lung, (**i**) heart, (**j**) kidney (magnification, × 200 for all panels).

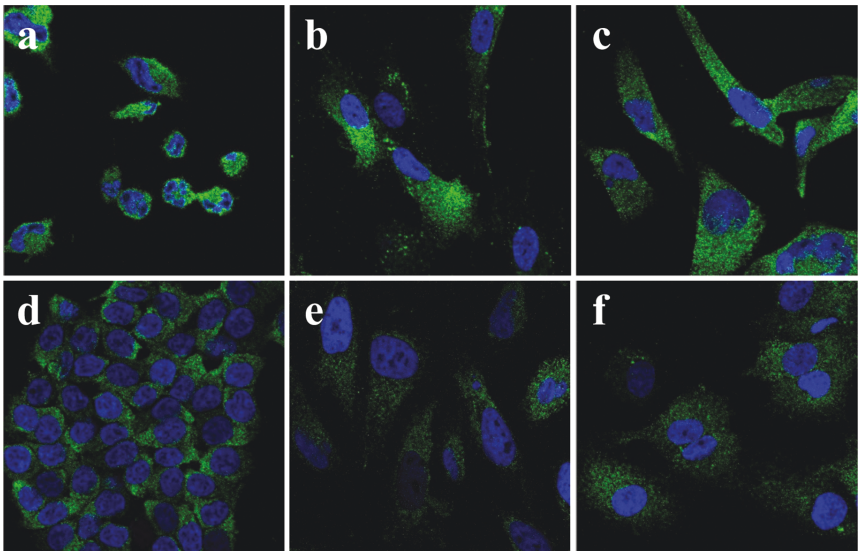

Figure 5. Confocal fluorescence microscopic detection of immunoreactive ANGT_HUMAN[448–462] in human cells in culture. THP1-derived macrophages (a), HAoEC (b), RD (c), HCT116 (d), HeLa (e), and HUEhT-1 (f) were stained with anti-ANGT_HUMAN[448–462] at 1:1000 dilution and reacted with Alexa Fluor 488 goat anti-rabbit IgG (magnification, × 63). Nuclei were counterstained with DAPI (blue).

be processed into ANGT_HUMAN[448–462] peptides in human cells.

To accurately determine the plasma levels of ANGT_HUMAN[448–462], a stable isotope-labeled ANGT_HUMAN[448–462] peptide was spiked into the human plasma samples prior to extraction and the XIC intensities were generated and extrapolated using an ultra-high-resolution liquid chromatography mass spectrometry method (Fig. 8). The plasma concentration of ANGT_HUMAN[448–462] extrapolated from the XICs generated by the endogenous peptide and reference peptides was approximately 10 nM. A raw data file of LC-MS/MS including the MS spectrum and XIC was deposited in the ProteomeXchange Consortium (http://proteomecentral.proteomexchange.org) via the jPOST partner repository (http://jpostdb.org) with the dataset identifier PXD033455 for ProteomeXchange and JPST001570 for jPOST [41].

Anorexigenic Activities of ANGT_HUMAN[448–462]

Sequence comparison of human and other mammalian angiotensinogen proteins revealed that the sequences corresponding to ANGT_HUMAN[448–462] are highly homologous among species (Table 3). Furthermore, ANGT_HUMAN[448–462] binds to ATP synthase expressed on the surfaces of human cells in culture and to the rat cerebral β-subunit of ATP synthase. Therefore, we investigated whether intracerebroventricular and intraperitoneal administration of ANGT_HUMAN[448–462] modulated spontaneous mouse behavior, including eating, drinking, and locomotor activities. Mice were intraperitoneally injected prior to the start of the dark phase and were continuously monitored throughout the dark phase [24, 25]. ANGT_HUMAN[448–462] suppressed food intake after intraperitoneal injection of 30 to 300 pmol/mouse (ANOVA, $P < 0.0001$, Fig. 9a). At 100 to 300 pmol/mouse, this peptide suppressed water intake and significantly stimulated spontaneous locomotor activity (Fig. 9a). ANGT_HUMAN[448–462] was then administered centrally to mice implanted with intracerebroventricular cannulas and provided free access to standard rodent chow and tap water. A single, very low dose of ANGT_HUMAN[448–462] significantly suppressed food and water intake without affecting locomotor activity. The cumulative food intake of mice receiving 1 pmol ANGT_HUMAN[448–462] remained low throughout the 12-hour dark phase (ANOVA, $P < 0.0001$, Fig. 9b). The central effect of ANGT_HUMAN[448–462] on the suppression of food intake was observed at 10 and 100 fmol/mouse,

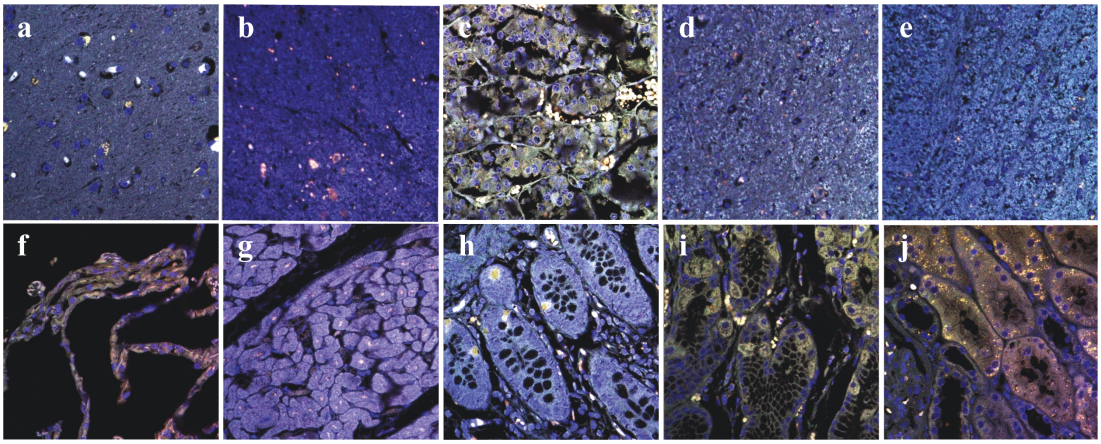

Figure 6. Co-localization of ANGT_HUMAN[448–462] and angiotensin II in human tissues. Confocal fluorescence microscopic detection of immunoreactive ANGT_HUMAN[448–462] and angiotensin II in human tissue array sections double-stained with the rabbit polyclonal anti-ANGT_HUMAN[448–462] and the mouse monoclonal anti-angiotensin II/III at 1:1000 and 1:500 dilution, respectively. The signals by ANGT_HUMAN[448–462] obtained with the Alexa Fluor 594 secondary antibody and those of angiotensin II obtained with the Alexa Fluor 488 secondary antibody were overlaid, resulting in yellow signals indicative of co-localization. The nuclei were counterstained with DAPI. (a) cerebral cortex, (b) medulla oblongata, (c) pituitary gland, (d) mid brain, (e) pons, (f) lung, (g) heart, (h) colon, (i) stomach, (j) renal tubules.

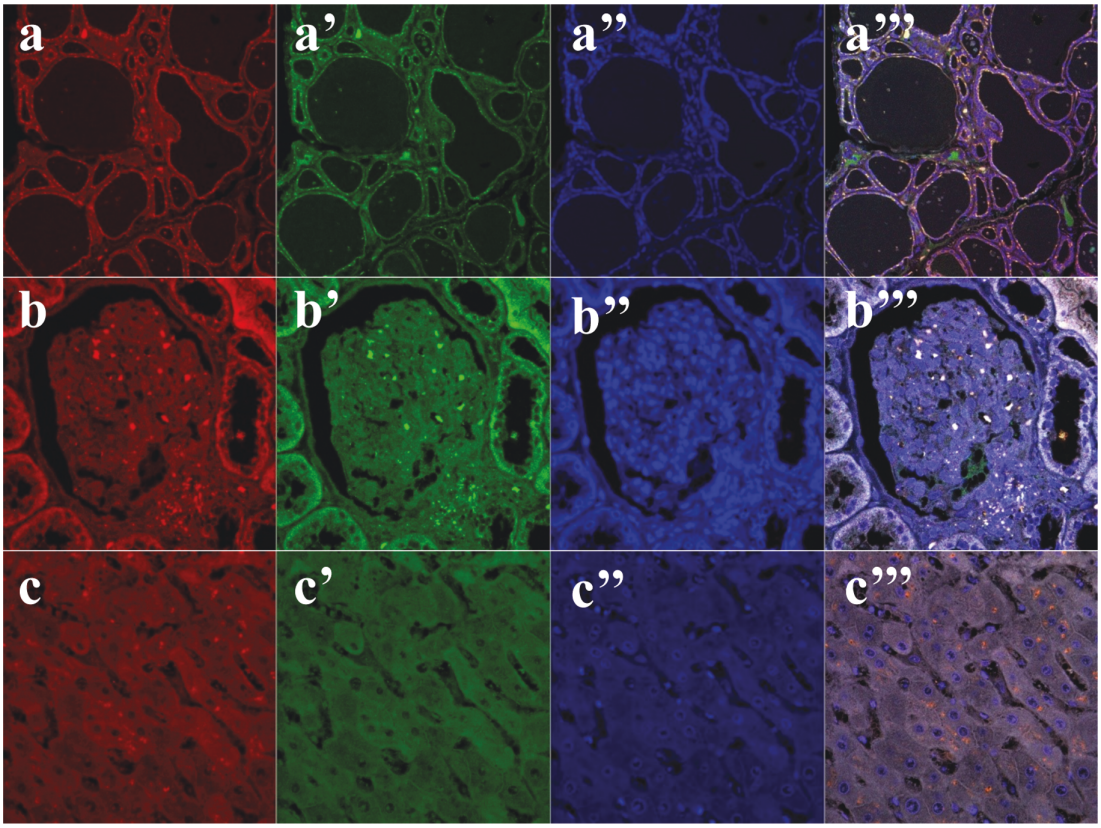

Figure 7. Distinct localization of ANGT_HUMAN[448–462] and angiotensin II in human tissues. Confocal fluorescence microscopic images of human tissue array sections double-stained with the rabbit polyclonal anti-ANGT_HUMAN[448–462] and the mouse monoclonal anti-angiotensin II/III at 1:1000 and 1:500 dilution, respectively. The red signals corresponding to the localization of angiotensin II were obtained with the Alexa Fluor 594 secondary antibody and the green signals representing ANGT_HUMAN[448–462] were obtained with the Alexa Fluor 488 secondary antibody. The nuclei were counterstained with DAPI (blue). Overlay resulted in yellow signals indicative of co-localization. (a–a‴) thyroid, (b–b‴) renal glomerulus, (c–c‴) liver (magnification, × 40 for all panels).

without affecting locomotor activity (ANOVA, $P < 0.0001$, Fig. 9c). Of the 135 synthetic peptides that were initially screened for their activities in cultured cells, 94 peptides were administered centrally, and spontaneous feeding, drinking, or locomotor activities of mice were determined using the same range of peptide doses and the same monitoring system; however, none caused any significant effects on feeding, drinking, or locomotor activities. These results indicate that ANGT_HUMAN[448–462] is an endogenous anorexigenic peptide present in human plasma.

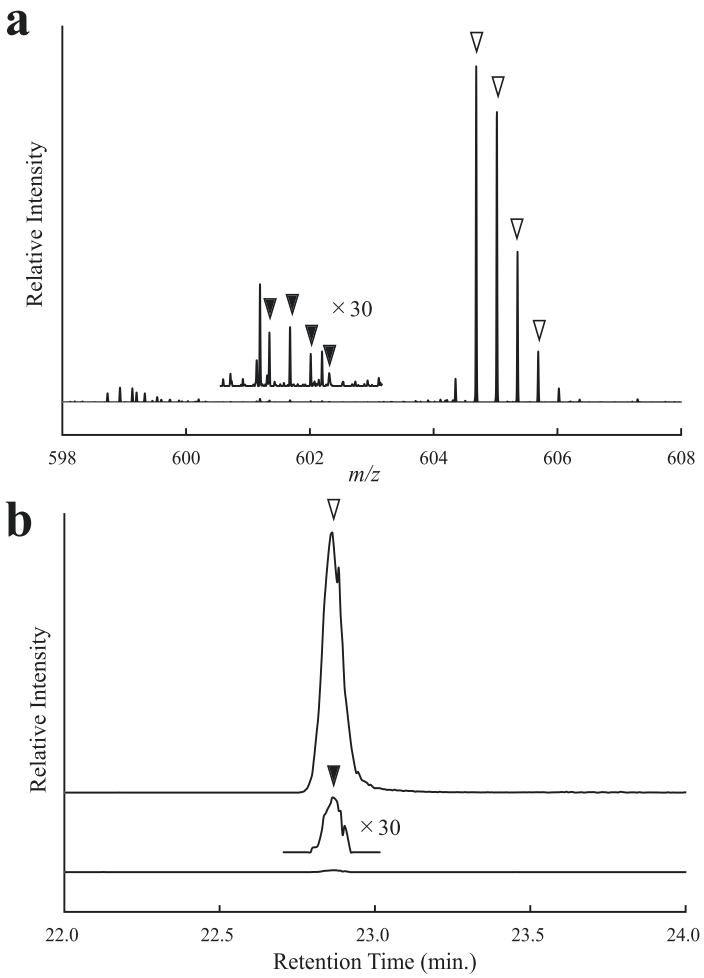

Figure 8. Quantitative analysis of the plasma ANGT_HUMAN[448–462] peptide using LC-MS/MS. The stable isotope-labeled peptide was spiked into human plasma at the final concentration of 2 nM, enriched using the modified differential solubilization method as described in the Methods and extracted peptides were separated by RP-HPLC and analyzed by LC-MS/MS. (a) MS spectrum of trivalent ions observed at retention time 22.81–22.92 minutes (indicated by triangles in b). Closed triangles represent those derived from the endogenous AGT_HUMAN[448–462] (*m/z* = 601.3452, 601.6795, 602.0138, 602.3481) and open triangles from the synthetic stable isotope-labeled peptide (*m/z* = 604.6876, 605.0219, 605.3562, 605.6905). (b) Comparison of the trivalent ion XICs with ± 6 ppm mass window of the stable isotope-labeled peptide (upper panel) and the endogenous peptide (lower panel). Total XIC area, defined as the sum of 3 ion precursors; monoisotopic mass (M), XICs of the first isotope peak (M + 1) and the second isotope peak (M + 2), was used to extrapolate plasma AGT_HUMAN[448–462] levels.

Discussion

We have discovered a novel anorectic peptide hormone, which we designated ANGT_HUMAN[448–462], by utilizing the large-scale native peptide resource we previously identified using our plasma peptidomic approach [5]. To estimate the potential biological functions of ANGT_HUMAN[448–462], which showed significant cell surface binding to several cultured cells, we attempted to identify its cell surface binding proteins using the following strategies. First, the fluorescence-labeled ANGT_HUMAN[448–462] peptide was reacted with cell- and tissue-derived lysates and electrophoresed using CN-PAGE, which allows the migration of high-molecular-weight protein complexes in their native state without dissociating peptides from their carrier proteins/receptors [12, 42, 43]. The fluorescence-positive bands detected were in-gel digested and analyzed using LC-MS/MS. Second, living cells in culture were incubated with biotinylated ANGT_HUMAN[448–462] peptide and, after treatment with a cross-linking reagent, cell lysates containing biotinylated peptide-bound cell proteins were analyzed by immunoblotting to confirm the bound proteins. All independent experiments performed using cultured cells and animal brain tissues revealed the presence of the β-subunit of ATP synthase in the extracted protein fractions containing the ANGT_HUMAN[448–462] peptide. Our current attempts enabled direct retrieval of cell surface proteins bound to the labeled peptidic ligands and subsequent identification of their binding proteins, although the overall usefulness of this approach to unravel receptors of peptidic ligands requires further investigation.

ATP synthase, expressed on the surface of certain cell types, mediates angiogenesis and cytosolic lipid accumulation of high-molecular-weight proteins, such as angiostatin [34, 35, 44] and apolipoprotein A-I [29]. Peptidic ligands also act on the β-subunit of ATP synthase to mediate eating and drinking behaviors in animals [11, 25, 45-47]. These results prompted us to investigate the effects of ANGT_HUMAN[448–462] on food and water intake. Central administration of ANGT_HUMAN[448–462] suppressed food intake in mice under voluntary free-feeding conditions at doses of 10 to 100 fmol.

Table 3. Amino acid sequence alignment of selected mammalian species of the peptides corresponding to ANGT_HUMAN[448–462]

Species	Sequence
Homo sapiens	KPEVLEVTLNRPFLF
Gorilla gorilla	KPEVLEVTLNRPFLF
Pan troglogytes	KPEVLEVTLNRPFLF
Rattus norvegicus	SPEVLDVTLSSPFLF
Mus musculus	SPEALDVTLSSPFLF
Bos taurus	GPEALEVTLNSPFLL
Ovis aries	GPEALEVTLNSPFLL

The incretin peptide, GLP-1, reduces food intake and body weight, and its receptor agonists have been successfully used worldwide for the treatment of diabetes. In mouse models, intracerebroventricular administration of 1 nmol GLP-1 reportedly reduced food intake [48], whereas another incretin peptide, GIP, required a larger dose (6 nmol) to suppress food intake [48]. Angiotensin II, C-type natriuretic peptide, and oxytocin decreased feeding after intracerebroventricular administration of 0.1 to 1 nmol, 1.5 nmol, and 1.0 nmol, respectively [49-51]. Central administration of leptin has been shown to induce satiety effects at a low dose of 30 pmol [52]. Although the experimental system used in this study could detect changes in eating behavior more sensitively than previously used models, our current results still indicate the anorectic potency of ANGT_HUMAN[448–462].

The peripheral anorectic effects of ANGT_HUMAN[448–462] were not as remarkable as their central effects and may not be as potent as that of a peripheral anorectic peptide, SBSN_HUMAN[279–295], which we recently identified [5]. It should be noted that central suppression of feeding was accompanied by reduced water intake, while peripheral administration was accompanied by increased spontaneous locomotor activity (Fig. 9a). Hunger and thirst circuits that involve AGRP and SFONOS1 neurons are considered discrete interoceptive pathways for distinct physiological states [53, 54]. Recently, however, glutamatergic neurons in the anterior peri-locus coeruleus have been identified as a polysynaptic convergence region in hunger and thirst behaviors that controls eating and drinking by regulating palatability during the consummatory phase of behavior [55]. Thus, suppression of food intake by ANGT_HUMAN[448–462] could be accompanied by reduced water intake, even without the direct action of the peptide. Some anorexic peptides may promote locomotor activity depending on the route and time of administration [56], whereas the interaction between the suprachiasmatic nucleus and the arcuate nucleus of the hypothalamus contributes to the regulation of food intake and locomotor activity during circadian variation [57]. Thus, the central interaction between feeding, drinking, and locomotor activity may be associated with the biological activities of anorectic peptides, although the exact mechanisms are still poorly understood.

The present study could not unravel the signal transduction pathways mediating ANGT_HUMAN[448–462]-induced anorectic effects. Recent studies have revealed that voltage-gated calcium channels are functionally coupled to F_1-ATP synthase to mediate external stimuli that induce extracellular Ca^{2+} influx in neutrophils [58]. Our results show that ANGT_HUMAN[448–462] acts on the cell surface ATP synthase β-subunit to induce extracellular calcium influx. However, because this effect was elicited by very high peptide doses and only in a limited type of cells, Ca^{2+} influx is an unlikely mechanism for the ANGT_HUMAN[448–462]-mediated anorexic effect. Major ligands of ATP synthase, such as angiostatin and enterostatin, exert their effects by altering ATP production [34-37]. The peripheral mechanism for F_1Fo ATP synthase agonists to suppress food intake involves an afferent vagal signaling pathway to the hypothalamic centers [59], while the central response is thought to be mediated through the induction of an increased protein gradient and augmented thermogenesis [36, 60, 61], which could act as a satiety signal to terminate the meal [62-64] or via pathways including serotonergic and κ-opioidergic components [65]. Further studies are needed to establish the exact mechanisms mediated by F_1Fo ATP synthase for ANGT_HUMAN[448–462]-induced anorectic effects.

ANGT_HUMAN[448–462] is located near the C-terminus end of its 485-amino-acid preproprotein, angiotensinogen, a precursor of the well-known vasoconstrictor, angiotensin II. Several bioactive angiotensin peptides, including angiotensin II, are biosynthesized from a decapeptide, angiotensin I, which is located immediately near the C-terminal of its 33 amino-acid signal peptide and cleaved from angiotensinogen by an enzyme, renin. The removal of angiotensin I is speculated to leave a protein termed des(angiotensinI) angiotensinogen, which has no known biological properties or fate. Our peptidomics analysis identified the presence of a variety of angiotensinogen-derived cleavage peptides in plasma with the highest confidence probability of an FDR of 0% [5] (Fig. 1a), including ANGT_HUMAN[448–485] and ANGT_HUMAN[463–485]. The former, ANGT_HUMAN[448–485], is considered to be an immediate precursor of ANGT_HUMAN[448–462], whereas the latter, ANGT_HUMAN[463–485], is the other cleaved product. Furthermore, the latest sequence information in the UniProt database reveals that there are no known splicing variants or potential isoforms predicted in the C-terminal region of the ANGT_HUMAN protein. Taken together, these results suggest the existence of an unidentified processing enzyme responsible for the biosynthesis of ANGT_HUMAN[448–462].

ANGT_HUMAN[448–462]-like immunoreactivity is present in many major human organs, including those of the central nervous, cardiovascular, and digestive systems and the kidney, in addition to cultured human macrophages, endothelial cells, and epithelial cells. The systemic localization of the ANGT_HUMAN[448–462] peptide was in good agreement with the systemic expression profiles of angiotensinogen mRNA [66-69] and tissue distribution of the precursor angiotensinogen protein [70, 71], which is also present in the plasma and cerebrospinal fluid [72]. We also succeeded in accurately determining the plasma level of this peptide to be approximately 10 pM. Although the level was lower than most other human peptide hormones, it is expected to play a physiological role, given the very low dose required to induce anorexic effects. To ensure accuracy in extrapolating the plasma concentration, we used the sums of the XIC areas of the 3 isotope peaks of precursor ions generated by high-resolution Orbitrap MS of plasma samples pre-spiked with serially diluted stable-isotope-labeled synthetic peptides. Because the data-dependent MS/MS analysis of the precursor

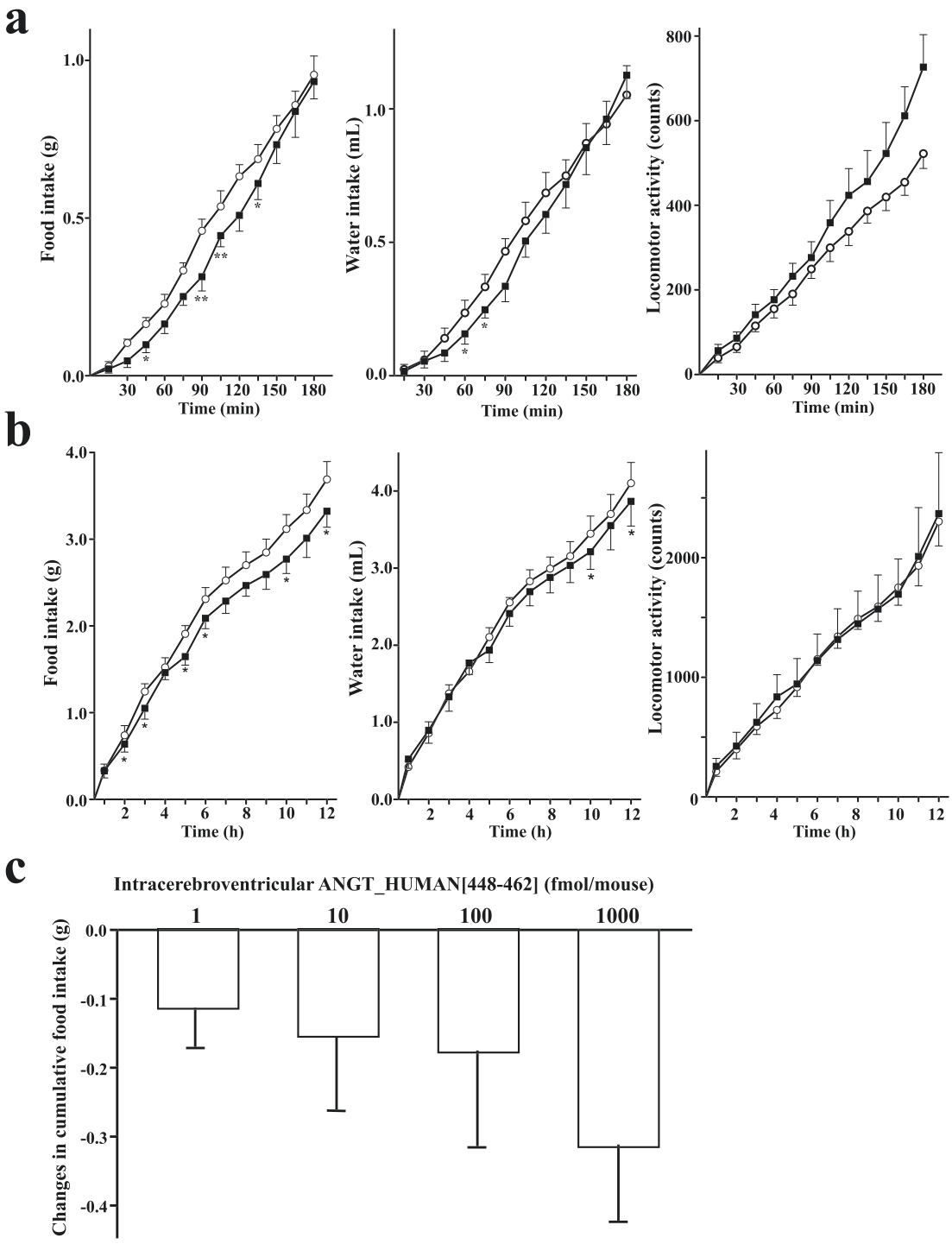

Figure 9. Biological activities of ANGT_HUMAN[448–462] on feeding, drinking, and locomotor behaviors in mice. (a) Synthetic ANGT_HUMAN[448–462] was intraperitoneally injected to ad libitum watered and fed mice at approximately 30 minutes before the onset of the dark phase, and cumulative food/water intake and locomotor activities were monitored throughout the entire dark phase of the diurnal cycle. Cumulative food and water intake are expressed in grams and in mL, and physical activity data in infrared beam interruption counts in mice treated without (open circle), or with 100 pmol/mouse ANGT_HUMAN[448–462] (closed square) during the initial 180 minutes period. $*P < 0.05$, $**P < 0.01$ compared with control experiments. (n = 4–7 mice per group). (b) Synthetic ANGT_HUMAN[448–462] at 1 pmol/mouse was centrally injected via an implanted intracerebroventricular cannulas, and cumulative food and water intake, and locomotor activities were recorded throughout the entire dark phase. $*P < 0.05$ compared with control experiments. (c) Changes in cumulative food intake of mice at the end of the 12 hours dark phase after central administration of 1, 10, 100, and 1000 fmol/mouse of ANGT_HUMAN[448–462] compared with that of the control mice. Data are expressed as mean ± SEM (n = 6–7 mice per group).

ion consistently identified the ANGT_HUMAN[448–462] peptide with a false discovery rate of 0%, the method only detected amino acid sequences identical to the synthetic ANGT_HUMAN[448–462], eliminating any possibility that it cross-reacted with unspecific sequences. The presence of ANGT_HUMAN[448–462] in human blood and a variety of human organs and tissues suggests its potential involvement in the maintenance of homeostasis and disease pathophysiology.

One of the central foci of translational proteomics is the identification of bioactive peptides and clinical biomarkers in biological samples. However, the enrichment of low-molecular-weight native peptides to generate high-quality mass spectra using human plasma has been extremely challenging because plasma contains an extraordinarily dynamic range of high-molecular-weight proteins. Our previous success in developing the high-yield plasma extraction technique [3, 4] and comprehensive identification of a large-scale plasma native peptide resource enabled the construction of an orphan peptidic ligand library [5], which is available for the identification of bioactive peptides with biological activities of interest for target-based modalities. Utilizing detailed mass spectrometry data of plasma native peptide sequences deposited into the ProteomeXchange Consortium via the PRoteomics IDEntifications (PRIDE) partner repository, we synthesized peptides of identified sequences, initiated functional screening studies in cultured human cells, and recently identified new bioactive peptides. In a previous study, we examined whether these synthetic peptides elicited significant intracellular responses in cultured cells [5]. The biological functions of peptides that stimulate potent intracellular signaling cascades can be estimated, and subsequent functional validation experiments can be designed. However, many bioactive peptides utilize cell surface non-G protein-coupled receptor proteins as their functional receptors and do not easily activate assayable cellular signaling pathways. The current methodology described herein retrieved cell surface target proteins by utilizing the binding capabilities of the peptidic ligand irrespective of the downstream intracellular signaling pathways or types of receptors and presents an alternative approach to estimate the biological activities of "orphan peptidic ligands".

In summary, we report the discovery of an anorectic peptide, designated ANGT_HUMAN[448–462], by exploring the human native peptide resource identified using plasma peptidomics. We identified its cell surface-binding protein as the β-subunit of ATP synthase, which is known to mediate eating and drinking behaviors in animals. ANGT_HUMAN[448–462] has a common precursor protein, angiotensinogen. The effective doses to suppress food intake after intracerebroventricular administration in mice were 10–1000 fmol, which were lower than those of other previously described anorectic peptide hormones. We expect that the current successful attempt to identify both bioactive peptides and their cell surface target proteins from our "orphan ligand library" obtained using human plasma peptidomics will facilitate the discovery of bioactive peptides and biomarkers and ultimately promote drug discovery research.

Acknowledgments

The authors thank Yukiko Kato for her technical assistance.

Financial Support

This work was funded by JSPS KAKENHI Grant Numbers JP18H05383 and 20K20389 to M.S. and 17H02206 and JP17K19926 to Y.K., by a grant from the All Kitasato Project Study to Y.K. and M.S., and by a Grant-in-Aid for Young Researchers from the Kitasato University Alumni Association and Parents' Association Grant of Kitasato University School of Medicine to K.O. The funders had no role in the study design, data collection or analysis, decision to publish, or preparation of the manuscript. No additional external funding was received for this study.

Author Contributions

Y.K. and M.S. analyzed and selected peptide sequences identified using plasma peptidomics and synthesized peptides for functional analyses. S.S. studied the effects of synthetic peptides on cellular responses and performed binding experiments. S.S. and M.I. retrieved peptide-bound proteins and performed LC-MS/MS analysis under the supervision of Y.K. K.O. performed mouse behavior experiments under supervision by M.S. M.I. designed and supervised the isolation experiment using rat brain tissue and cross-linking reagent. M.S. designed and raised specific antibodies and S.S. performed immunohistochemistry and immunofluorescence under supervision by M.S. M.S. conceived and designed the entire study, analyzed the data, and wrote the manuscript. All authors discussed the results and commented on the manuscript.

Disclosures/Conflict of Interest

Y.K. and M.S. are co-inventors of patents relevant to this work, which should therefore be declared as competing financial interests. The rest of the authors declare no conflicts of interest.

Data Availability

Some or all data generated or analyzed during this study are included in this published article or in the data repositories listed in References.

References

1. Anderson NL, Anderson NG. The human plasma proteome: history, character, and diagnostic prospects. *Mol Cell Proteomics*. 2002;1(11):845-867. doi:10.1074/mcp.r200007-mcp200
2. Tirumalai RS, Chan KC, Prieto DA, Issaq HJ, Conrads TP, Veenstra TD. Characterization of the low molecular weight human serum proteome. *Mol Cell Proteomics*. 2003;2(10):1096-1103. doi:10.1074/mcp.M300031-MCP200
3. Kawashima Y, Fukutomi T, Tomonaga T, *et al*. High-yield peptide-extraction method for the discovery of subnanomolar biomarkers from small serum samples. *J Proteome Res*. 2010;9(4):1694-1705. doi:10.1021/pr9008018
4. Saito T, Kawashima Y, Minamida S, *et al*. Establishment and application of a high- quality comparative analysis strategy for the discovery and small-scale validation of low-abundance biomarker peptides in serum based on an optimized novel peptide extraction method. *J Electrophoresis*. 2013;57(1):1-9. doi:10.2198/jelectroph.57.1
5. Taguchi T, Kodera Y, Oba K, *et al*. Suprabasin-derived bioactive peptides identified by plasma peptidomics. *Sci Rep*. 2021;11(1):1047. doi:10.1038/s41598-020-79353-4
6. Vizcaino JA, Deutsch EW, Wang R, *et al*. ProteomeXchange provides globally coordinated proteomics data submission and dissemination. *Nat Biotechnol*. 2014;32(3):223-226. doi:10.1038/nbt.2839
7. Nakai K, Horton P. PSORT: a program for detecting sorting signals in proteins and predicting their subcellular localization. *Trends Biochem Sci*. 1999;24(1):34-36. doi:10.1016/s0968-0004(98)01336-x.

8. Shichiri M, Hirata Y, Nakajima T, *et al*. Endothelin-1 is an autocrine/paracrine growth factor for human cancer cell lines. *J Clin Invest*. 1991;87(5):1867-1871. doi:10.1172/JCI115210
9. Shichiri M, Ishimaru S, Ota T, Nishikawa T, Isogai T, Hirata Y. Salusins: newly identified bioactive peptides with hemodynamic and mitogenic activities. *Nat Med*. 2003;9(9):1166-1172. doi:10.1038/nm913
10. Tani Y, Yamada S, Inoshita N, Hirata Y, Shichiri M. Regulation of growth hormone secretion by (pro)renin receptor. *Sci Rep*. 2015;5:10878. doi:10.1038/srep10878
11. Shichiri M, Nonaka D, Lee LJ, Tanaka K. Identification of the salusin-β receptor using proteoliposomes embedded with endogenous membrane proteins. *Sci Rep*. 2018;8(1):17865. doi:10.1038/s41598-018-35740-6
12. Hoshiyama A, Fujimoto K, Konno R, *et al*. Identification of plasma binding proteins for glucose-dependent insulinotropic polypeptide. *Endocr J*. 2019;66(7):621-628. doi:10.1507/endocrj.EJ18-0472
13. Satoh M, Haruta-Satoh E, Omori A, *et al*. Effect of thyroxine on abnormal pancreatic proteomes of the hypothyroid rdw rat. *Proteomics*. 2005;5(4):1113-1124. doi:10.1002/pmic.200401117
14. Rappsilber J, Ishihama Y, Mann M. Stop and go extraction tips for matrix-assisted laser desorption/ionization, nanoelectrospray, and LC/MS sample pretreatment in proteomics. *Anal Chem*. 2003;75(3):663-670. doi:10.1021/ac026117i
15. Suzuki S, Kodera Y, Saito T, *et al*. Methionine sulfoxides in serum proteins as potential clinical biomarkers of oxidative stress. *Sci Rep*. 2016;6:38299. doi:10.1038/srep38299
16. Eng JK, McCormack AL, Yates JR. An approach to correlate tandem mass spectral data of peptides with amino acid sequences in a protein database. *J Am Soc Mass Spectrom*. 1994;5(11):976-989. doi:10.1016/1044-0305(94)80016-2
17. Fujimoto K, Hayashi A, Kodera Y, *et al*. Identification and quantification of plasma free salusin-β, an endogenous parasympathomimetic peptide. *Sci Rep*. 2017;7(1):8275. doi:10.1038/s41598-017-08288-0
18. Hong S, Pedersen PL. ATP synthase and the actions of inhibitors utilized to study its roles in human health, disease, and other scientific areas. *Microbiol Mol Biol Rev*. 2008;72(4):590-641. doi:10.1128/MMBR.00016-08
19. Kawashima Y, Satoh M, Saito T, *et al*. Cyclic sample pooling using two-dimensional liquid chromatography system enhances coverage in shotgun proteomics. *Biomed Chromatogr*. 2013;27(6):691-694. doi:10.1002/bmc.2864
20. Masaki T, Kodera Y, Terasaki M, Fujimoto K, Hirano T, Shichiri M. GIP_HUMAN[22-51] is a new proatherogenic peptide identified by native plasma peptidomics. *Sci Rep*. 2021;11(1):14470. doi:10.1038/s41598-021-93862-w
21. Franke AA, Li X, Menden A, Lee MR, Lai JF. Oxytocin analysis from human serum, urine, and saliva by orbitrap liquid chromatography-mass spectrometry. *Drug Test Anal*. 2019;11(1):119-128. doi:10.1002/dta.2475
22. Momozono A, Kodera Y, Sasaki S, Nakagawa Y, Konno R, Shichiri M. Oxidised Met(147) of human serum albumin is a biomarker of oxidative stress, reflecting glycaemic fluctuations and hypoglycaemia in diabetes. *Sci Rep*. 2020;10(1):268. doi:10.1038/s41598-019-57095-2
23. Oba K, Hosono K, Amano H, *et al*. Downregulation of the proangiogenic prostaglandin E receptor EP3 and reduced angiogenesis in a mouse model of diabetes mellitus. *Biomed Pharmacother*. 2014;68(8):1125-1133. doi:10.1016/j.biopha.2014.10.022
24. Nakano-Tateno T, Shichiri M, Suzuki-Kemuriyama N, Tani Y, Izumiyama H, Hirata Y. Prolonged effects of intracerebroventricular angiotensin II on drinking, eating and locomotor behavior in mice. *Regul Pept*. 2012;173(1-3):86-92. doi:10.1016/j.regpep.2011.09.011
25. Suzuki-Kemuriyama N, Nakano-Tateno T, Tani Y, Hirata Y, Shichiri M. Salusin-β as a powerful endogenous antidipsogenic neuropeptide. *Sci Rep*. 2016;6:20988. doi:10.1038/srep20988
26. Kall L, Storey JD, MacCoss MJ, Noble WS. Posterior error probabilities and false discovery rates: two sides of the same coin. *J Proteome Res*. 2008;7(1):40-44. doi:10.1021/pr700739d
27. Pedersen PL. Transport ATPases into the year 2008: a brief overview related to types, structures, functions and roles in health and disease. *J Bioenerg Biomembr*. 2007;39(5-6):349-355. doi:10.1007/s10863-007-9123-9
28. Stock D, Gibbons C, Arechaga I, Leslie AG, Walker JE. The rotary mechanism of ATP synthase. *Curr Opin Struct Biol*. 2000;10(6):672-679. doi:10.1016/s0959-440x(00)00147-0
29. Arakaki N, Kita T, Shibata H, Higuti T. Cell-surface H+-ATP synthase as a potential molecular target for anti-obesity drugs. *FEBS Lett*. 2007;581(18):3405-3409. doi:10.1016/j.febslet.2007.06.041
30. Burrell HE, Wlodarski B, Foster BJ, *et al*. Human keratinocytes release ATP and utilize three mechanisms for nucleotide interconversion at the cell surface. *J Biol Chem*. 2005;280(33):29667-29676. doi:10.1074/jbc.M505381200
31. Das B, Mondragon MO, Sadeghian M, Hatcher VB, Norin AJ. A novel ligand in lymphocyte-mediated cytotoxicity: expression of the beta subunit of H+ transporting ATP synthase on the surface of tumor cell lines. *J Exp Med*. 1994;180(1):273-281. doi:10.1084/jem.180.1.273
32. Kim DW, Kim KH, Yoo BC, *et al*. Identification of mitochondrial F(1)F(0)-ATP synthase interacting with galectin-3 in colon cancer cells. *Cancer Sci*. 2008;99(10):1884-1891. doi:10.1111/j.1349-7006.2008.00901.x
33. Martinez LO, Jacquet S, Esteve JP, *et al*. Ectopic beta-chain of ATP synthase is an apolipoprotein A-I receptor in hepatic HDL endocytosis. *Nature*. 2003;421(6918):75-79. doi:10.1038/nature01250
34. Moser TL, Kenan DJ, Ashley TA, *et al*. Endothelial cell surface F1-F0 ATP synthase is active in ATP synthesis and is inhibited by angiostatin. *Proc Natl Acad Sci USA*. 2001;98(12):6656-6661. doi:10.1073/pnas.131067798
35. Moser TL, Stack MS, Asplin I, *et al*. Angiostatin binds ATP synthase on the surface of human endothelial cells. *Proc Natl Acad Sci USA*. 1999;96(6):2811-2816.
36. Berger K, Sivars U, Winzell MS, *et al*. Mitochondrial ATP synthase--a possible target protein in the regulation of energy metabolism in vitro and in vivo. *Nutr Neurosci*. 2002;5(3):201-210. doi:10.1080/10284150290008604
37. Berger K, Winzell MS, Mei J, Erlanson-Albertsson C. Enterostatin and its target mechanisms during regulation of fat intake. *Physiol Behav*. 2004;83(4):623-630. doi:10.1016/j.physbeh.2004.08.040
38. Park M, Lin L, Thomas S, *et al*. The F1-ATPase beta-subunit is the putative enterostatin receptor. *Peptides*. 2004;25(12):2127-2133. doi:10.1016/j.peptides.2004.08.022
39. White CL, Bray GA, York DA. Intragastric beta-casomorphin(1-7) attenuates the suppression of fat intake by enterostatin. *Peptides*. 2000;21(9):1377-1381. doi:10.1016/s0196-9781(00)00281-3
40. Lin L, Umahara M, York DA, Bray GA. Beta-casomorphins stimulate and enterostatin inhibits the intake of dietary fat in rats. *Peptides*. 1998;19(2):325-331. doi:10.1016/s0196-9781(97)00307-0
41. Okuda S, Watanabe Y, Moriya Y, *et al*. jPOSTrepo: an international standard data repository for proteomes. *Nucleic Acids Res*. 2017;45(D1):D1107-D1111. doi:10.1093/nar/gkw1080
42. Pfeiffer K, Gohil V, Stuart RA, *et al*. Cardiolipin stabilizes respiratory chain supercomplexes. *J Biol Chem*. 2003;278(52):52873-52880. doi:10.1074/jbc.M308366200
43. Wittig I, Schagger H. Advantages and limitations of clear-native PAGE. *Proteomics*. 2005;5(17):4338-4346. doi:10.1002/pmic.200500081
44. Wahl ML, Kenan DJ, Gonzalez-Gronow M, Pizzo SV. Angiostatin's molecular mechanism: aspects of specificity and regulation elucidated. *J Cell Biochem*. 2005;96(2):242-261. doi:10.1002/jcb.20480
45. Lin L, Chen J, York DA. Chronic ICV enterostatin preferentially reduced fat intake and lowered body weight. *Peptides*. 1997;18(5):657-661. doi:10.1016/s0196-9781(97)00128-9

46. Mei J, Erlanson-Albertsson C. Effect of enterostatin given intravenously and intracerebroventricularly on high-fat feeding in rats. *Regul Pept*. 1992;41(3):209-218.
47. Okada S, York DA, Bray GA, Mei J, Erlanson-Albertsson C. Differential inhibition of fat intake in two strains of rat by the peptide enterostatin. *Am J Physiol*. 1992;262(6 Pt 2):R1111-R1116. doi:10.1152/ajpregu.1992.262.6.R1111
48. NamKoong C, Kim MS, Jang BT, Lee YH, Cho YM, Choi HJ. Central administration of GLP-1 and GIP decreases feeding in mice. *Biochem Biophys Res Commun*. 2017;490(2):247-252. doi:10.1016/j.bbrc.2017.06.031
49. Ohinata K, Fujiwara Y, Fukumoto S, Iwai M, Horiuchi M, Yoshikawa M. Angiotensin II and III suppress food intake via angiotensin AT(2) receptor and prostaglandin EP(4) receptor in mice. *FEBS Lett*. 2008;582(5):773-777. doi:10.1016/j.febslet.2008.01.054
50. Yamada-Goto N, Katsuura G, Ebihara K, *et al*. Intracerebroventricular administration of C-type natriuretic peptide suppresses food intake via activation of the melanocortin system in mice. *Diabetes*. 2013;62(5):1500-1504. doi:10.2337/db12-0718
51. Zhang G, Cai D. Circadian intervention of obesity development via resting-stage feeding manipulation or oxytocin treatment. *Am J Physiol*. 2011;301(5):E1004-E1012.
52. Brown LM, Clegg DJ, Benoit SC, Woods SC. Intraventricular insulin and leptin reduce food intake and body weight in C57BL/6J mice. *Physiol Behav*. 2006;89(5):687-691. doi:10.1016/j.physbeh.2006.08.008
53. Saper CB, Chou TC, Elmquist JK. The need to feed: homeostatic and hedonic control of eating. *Neuron*. 2002;36(2):199-211. doi:10.1016/s0896-6273(02)00969-8
54. Betley JN, Xu S, Cao ZFH, *et al*. Neurons for hunger and thirst transmit a negative-valence teaching signal. *Nature*. 2015;521(7551):180-185. doi:10.1038/nature14416
55. Gong R, Xu S, Hermundstad A, Yu Y, Sternson SM. Hindbrain double-negative feedback mediates palatability-guided food and water consumption. *Cell*. 2020;182(6):1589-1605.e22. doi:10.1016/j.cell.2020.07.031
56. Schroeder LE, Leinninger GM. Role of central neurotensin in regulating feeding: Implications for the development and treatment of body weight disorders. *Biochim Biophys Acta Mol Basis Dis*. 2018;1864(3):900-916. doi:10.1016/j.bbadis.2017.12.036
57. Mendez-Hernandez R, Escobar C, Buijs RM. Suprachiasmatic nucleus-arcuate nucleus axis: interaction between time and metabolism essential for health. *Obesity (Silver Spring)*. 2020;28(Suppl 1):S10-S17. doi:10.1002/oby.22774
58. Zhu B, Feng Z, Guo Y, *et al*. F0F1 ATP synthase regulates extracellular calcium influx in human neutrophils by interacting with Cav2.3 and modulates neutrophil accumulation in the lipopolysaccharide-challenged lung. *Cell Commun Signal*. 2020;18(1):19. doi:10.1186/s12964-020-0515-3
59. Tian Q, Nagase H, York DA, Bray GA. Vagal-central nervous system interactions modulate the feeding response to peripheral enterostatin. *Obes Res*. 1994;2(6):527-534. doi:10.1002/j.1550-8528.1994.tb00101.x
60. Chan CB. Endogenous regulation of insulin secretion by UCP2. *Clin Lab*. 2002;48(11-12):599-604.
61. Ookuma M, York DA. Inhibition of insulin release by enterostatin. *Int J Obes Relat Metab Disord*. 1998;22(8):800-805. doi:10.1038/sj.ijo.0800663
62. Brobeck JR. Effect of changes in pH, in osmolarity, or in temperature on food intake. *Am J Clin Nutr*. 1985;42(5 Suppl):951-955. doi:10.1093/ajcn/42.5.951
63. Friedman MI. Fuel partitioning and food intake. *Am J Clin Nutr*. 1998;67(3 Suppl):513S-518S. doi:10.1093/ajcn/67.3.513S
64. Himms-Hagen J. Role of brown adipose tissue thermogenesis in control of thermoregulatory feeding in rats: a new hypothesis that links thermostatic and glucostatic hypotheses for control of food intake. *Proc Soc Exp Biol Med*. 1995;208(2):159-169. doi:10.3181/00379727-208-43847a
65. Ookuma K, Barton C, York DA, Bray GA. Effect of enterostatin and kappa-opioids on macronutrient selection and consumption. *Peptides*. 1997;18(6):785-791. doi:10.1016/s0196-9781(97)00029-6
66. Lynch KR, Peach MJ. Molecular biology of angiotensinogen. *Hypertension*. 1991;17(3):263-269. doi:10.1161/01.hyp.17.3.263
67. Morgan L, Broughton Pipkin F, Kalsheker N. Angiotensinogen: molecular biology, biochemistry and physiology. *Int J Biochem Cell Biol*. 1996;28(11):1211-1222. doi:10.1016/s1357-2725(96)00086-6
68. Phillips MI, Speakman EA, Kimura B. Levels of angiotensin and molecular biology of the tissue renin angiotensin systems. *Regul Pept*. 1993;43(1-2):1-20.
69. Rafatian N, Milne RW, Leenen FH, Whitman SC. Role of renin-angiotensin system in activation of macrophages by modified lipoproteins. *Am J Physiol*. 2013;305(9):H1309-H1320.
70. Bader M. Tissue renin-angiotensin-aldosterone systems: targets for pharmacological therapy. *Annu Rev Pharmacol Toxicol*. 2010;50:439-465. doi:10.1146/annurev.pharmtox.010909.105610
71. Thomas WG, Sernia C. Immunocytochemical localization of angiotensinogen in the rat brain. *Neuroscience*. 1988;25(1):319-341. doi:10.1016/0306-4522(88)90029-2
72. Ito T, Eggena P, Barrett JD, Katz D, Metter J, Sambhi MP. Studies on angiotensinogen of plasma and cerebrospinal fluid in normal and hypertensive human subjects. *Hypertension*. 1980;2(4):432-436. doi:10.1161/01.hyp.2.4.432